LIBRARY

C.P. No. 145
(15.243)
A.R.C. Technical Report

[illegible]

MINISTRY OF SUPPLY

AERONAUTICAL RESEARCH COUNCIL

CURRENT PAPERS

Zero Lift Drag Measurements on Swept Wings at Transonic and Supersonic Speeds using the Ground-launched Rocket-boosted Model Technique

By

T. Lawrence, B.Sc., B.E. and C. Kell, A.M.I.Mech.E.

LONDON: HER MAJESTY'S STATIONERY OFFICE

1954

Price 2s. 6d. net

C.P. No.145

Technical Note No. Aero.2161

May, 1952

ROYAL AIRCRAFT ESTABLISHMENT

Zero lift drag measurements on swept wings at transonic and supersonic speeds using the ground-launched rocket-boosted model technique

by

T. Lawrence, B.Sc., B.E.

and

C. Kell, A.M.I.Mech.E.

SUMMARY

This is mainly a documentary *record of drag* measurements on 14 swept wings varying in planform from deltas to swept untapered *wings*, and from 4% to 10% thick. The Reynolds number of the tests was 7×10^6 per foot chord at M = 1.0. The results are compared with theory for wings of double wedge section, and an attempt is made to check the validity of the supersonic similarity laws. Three preliminary conclusions are drawn.

(a) At supersonic speeds, the wave drag of a given wing varies as the square of the thickness ratio;

(b) the supersonic similarity law allows the drag of 'similar' wings to be compared; and

(c) there is some hope that the drag of round-nose section wings can be estimated from theoretical calculations of the drag of wings of double wedge section.

LIST OF CONTENTS

LIST OF TABLES

LIST OF ILLUSTRATIONS

1 Introduction

An earlier report' hasdescribed the development of the R.A.E. ground-launched, m&et-boosted model technique of measuring drag at transonic and low supersonic speeds The present note deals with the application of the technique to drag measurements at zero lift on a number of swept tapered and untapered wings. The experimental results are compared with theoretical estimates of the drag of wings of identical planform and double wedge section, and the validity of the supersonic similarity laws are checked.

2 Test vehicles

Full details of the test vehicles are given in Table i and Fig.1, and a typical example is illustrated in Fig.2.

The test vehicles were built around a solid fuel rocket of 5 inches diameter and 65 inches long. It had an impulse of about 6400 lb.secs and a burning time of about 1.8 secs. The weight of the test vehicles after the rocket had ceased burning varied from about 90 to 110 lb. The rocket case was enclosed in a body $6\frac{3}{8}$ inches diameter and 73 inches long, finished at the front end by a tangent ogive $25\frac{1}{2}$ inches long. At the rear end the standard body carried two stabilising fins, of which details are given in Fig.1. On this standard body were mounted, for most tests reported here, two wings 0f about 20 inches exposed. half span. On some vehicles, the body carried three half wings and the stabilising fins were omitted. Table I gives full details of all wings tested, including sufficient leading dimensions to allow the test vehicles, with the aid of Fig.1, to be reconstructed.

Further discoussion of the test vehicles, including typical surface finish measurements on body and wings, profile accuracy details, and the philosophy behind the vehicle layout. is given in Ref.1.

3 Method of test and analysis

The test *vehicles* were launched on an existing open air range? generally at an elevation of $13\frac{1}{2}^{\circ}$ to the horizontal. The vehicles in general rose to an altitude **of about** 1000 **feet,** and travelled **a distance** of about 15,000 feet. From the record of a reflection Doppler radar set mounted behind the launching apron, and the trajectory computed from kine-theodolites observations, the flight path velocity, flight path deceleration and inclination of the flight path to the horizontal were determined. Corrections for observed wind were applied to these results, and the drag computed. Full details of the computational methods are given in Ref.1.

4 Presentation of results

Referring to Table I, drag results are presented here for 3 swept untapered wings with streamwise tips (Models 1, 2 and 3) and 2 swept untapered wings with *out-off* tips* (Models 4 and 5), for 2 delta wings (Models 6 and 7) 4 cropped delta wings (Models 8, 9, 10 and II) and for 3swept tapered wings with streamwise tips which, according to the supersonic similarity laws, are similar (Models 12, 13 and 14). On most Of the models the section was RAE.101, 6% thick, hut in some cases both different sections and different thicknesses were used. On one wing (Model 11) the thickness ratio increased *towards* the *tips (see* Fig.4).

• i.e. out-Off at right angles to the line of flight. This planform has at times been referred to as "pseudo-delta" and "delta with cranked trailing edge."

In Figs.6 - 18, the drag of the models is presented. Referring to Fig.6 as a typical example, in Fig.6a is shown both the drag of the winged vehicle, and the drag of a wingless basic body, both as coefficients C_{D_B} based on the frontal area of the body. In Fig.6b, the difference between the curves in Fig.6a, i.e. the profile drag of the wings alone, together with any interference of the wings on the body and of the body on the wings, is expressed as the usual coefficient C_{D_o} based on exposed wing area. Fig.6b also shows the estimated friction drag, based on the mean chord of the wing (see Table I) and Fig.3 (see paragraph 5.2). Subsequently in Figs.20 - 25 the difference between these two curves, the wave drag coefficient C_{D_W}, is considered.

The vehicle drag was measured in decelerating flight, in most cases from about M = 1.4 to M = 0.85. An exception is Model 8; this model was designed specifically to cover the transonic region. On some models however, the vehicle drag measurements cease at about M = 1. In some cases this was because the wings fluttered off as transonic speeds were reached, in other cases the vehicle was of low drag and flew out of the Doppler beam before it had decelerated to subsonic velocities.

The Reynolds number of the tests was 7×10^6 per foot chord at M = 1.0, and varied linearly with Mach number. The mean chord of the wings is given in Table I, and Fig.5 shows the extreme variations in Reynolds number for all models. Drag measurements by the present technique are made in decelerating flight; for the models of this report average values of the deceleration were 4.5g at M = 1.5, and 1g at M = 0.9. Although there is an effect of acceleration on drag, theory shows that the effects of accelerations of these orders are negligible.

5 Discussion of results

5.1 Effect of vehicle layout

The relative merits of 2-winged and 3-winged vehicles have been argued previously[1]. Most of the tests reported in this paper have been on 2-winged vehicles. Some results using 3-winged vehicles are included here and summarised in Fig.19 and from them the effect of vehicle layout can be seen; in most cases there is an unfavourable interference drag on the 3-winged vehicles, and an earlier drag rise. On the swept untapered wing with cut-off tips, however (Models 4 and 5) there is a favourable interference, the drag from 3-winged vehicles being less than that from 2-winged vehicles for both RAE.101 and RAE.104 sections, below a Mach Number of about 1.45.

5.2 Skin friction

No direct measurements of either friction drag or transition point have been made. However, if comparisons between different wings, and comparisons with theory are to be attempted, some allowance for friction drag must be made. Previously (Ref.1) from the effect on drag of having a rough surface finish, it had been deduced that for the present Phenoglaze finish the transition must be far back on the wing. This is confirmed in the present series of tests by the fact that the measured subsonic drag is in every case less than the friction drag that would be estimated assuming transition at the nose of the aerofoil.

Most of these tests have been done on RAE.101 section wings, which at $C_L = 0$ have the maximum thickness and the commencement of the unfavourable pressure gradient at about 30% of the chord. Full scale and tunnel experience suggests that on sections of this type at $C_L \approx 0$ transition occurs just aft of the commencement of an unfavourable pressure gradient i.e. aft of 0.3c. Secondly, from the measured subsonic drag, and using Royal Aeronautical Society Data Sheets corrected for Mach number according to Cope[2] it is possible to deduce a transition point. Rejecting some anomalous results, the value[3] deduced from these tests, vary from about 0.3c to 0.5c, with a mean value of 0.39c. Finally, the Reynolds Number of transition, using these deduced transition points, varies from 2×10^6 to 4×10^6, which is in the range one would predict.

On this evidence therefore, it has been assumed that transition occurred on all models at 0.4c, and when comparing results friction drag as shown in Fig.3 has been subtracted.

It should be remembered that these deductions about the probable position of the transition point are based in the main on comparisons at subsonic speeds. Allowance has been made for the effect of Mach Number on the friction drag coefficient, but no account has been taken of the effect, if any, of Mach Number on transition point. In this respect the present procedure is open to criticism and possibly to later amendment.

5.3 Effect of thickness

Supersonic wing theory suggests that the wave drag is proportional to τ^2, and from the present results this can be checked in two instances. Model 13b had 3 wings of RAE.101 section 6% thick, whilst on Model 14 the 3 wings were of the same section and 10% thick. $\left(\frac{C_{D_W}}{\tau^2}\right)$ for these two wings are compared in Fig.20b, and considering the differences that would be made by small errors in estimating C_{D_f}, the agreement is considered satisfactory. As pointed out in Table I the wings of Model 11 varied in thickness from 0.04 at the root to 0.0765 at the tip (see Fig.4). Weighting the thickness ratio according to the local chord, we get

$$\bar{\tau} = \left[\int_0^s \tau^2 \, c \, dy \Big/ \int_0^s c \, . \, dy \right]^{\frac{1}{2}} = 0.0489$$

using this value of $\bar{\tau}$, $\left(\frac{C_{D_W}}{\bar{\tau}^2}\right)$ for Model 11 is compared in Fig.20a with that for Model 10 (same planform and section, 4% thick throughout). Again the comparison is very satisfactory, and these two checks suggest that the effects of changes in thickness can be estimated by this method.

5.4 Effect of section change

In the results presented here all wings were of round nose symmetrical section having, with one exception, the maximum thickness at 30 - 31% of the chord, Models 5, of RAE.104 section, had the maximum thickness at 42% of the chord. Comparison of the drags of Models 4 and 5 is made in Fig.19a, and two rather curious features demand comment. Firstly, as has been noted earlier, with this planform the wing drag

from 2-winged vehicles, on models of both RAE.101 and RAE.104 section, is greater than the wing drag measured on 3-winged vehicles; this is apparently a mutual interference effect. Secondly, on both 2 and 3-winged vehicles, the markedly different shapes of curve for RAE.101 and RAE.104 section is notable. Since the Mach number at which the drag rise occurs on the winged vehicles is very nearly that at which the drag rise occurs on the basic body alone, it is not possible to draw any useful conclusions about the drag below about M = 1. But above about M = 1.05 the accuracy of drag determination is good. No physical explanation is offered for the large hump in the drag curves of Models 4a ad 4b between Mach numbers of about 1.1 and 1.35. Thompson[3] has calculated the wave drag of a wing of double wedge section and this type of planform. He has also shown that, certainly between M = 1.1 and 1.5 for a wing of 60° leading edge sweep, a good approximation to the dmg can be obtained by considering the wing to consist of an isolated inboard untapered portion and an isolated outboard delta, the total drag being obtained by weighting these isolated drags according to their areas. Using this approximation and the curves of Ref.4, tine drags of wings of the same planform as Models 4 and 5 and of double wedge section, but with maximum thickness at 30% and 40%, have been estimated, and are shown in Fig.22. It is seen that these theoretical curves are consistent with theory for other wing planforms in putting the wing with the more forward maximum thickness position at the lower drag, until the maximum thickness line on the delta tip becomes sonic when, at "supersonic" speeds, the lover drag of the forebody on the section mth "sharper nose" (more aft maximum thickness position) outweighs all other effects.

5.5 Comparison With theory and with similarity laws

It would have been most valuable if from these tests any general conclusions could have been drawn about the drag in the transonic region, but for several reasons no such general conclusions are possible.

Firstly, the drag rise Mach number is of interest. In these experiments, however, the drag of the body alone begins to rise at about M = 0.95, so that in many vehicles the rise in drag of the wing is masked. This applies particularly for the thinner, more highly swept wings. Consequently no useful analysis of the drag rise Mach number is possible.

The drag at M = 1.0 would also be worth examination. A preliminary analysis suggests that in fact it will be possible to draw some general conclusions, but the results contained in this report alone are insufficient to verify then and they are held over for a more exhaustive analysis now to be attempted.

The supersonic similarity law for drag may be written

$$\frac{C_{D_W}}{A_\tau^2} = f\left[A\sqrt{M^2-1}\ ,\ A\tan\Lambda_{\frac{1}{2}}\ ,\ \lambda\ ,\ \text{section}\right]$$

Using this form, 3 recent note[4] has given a selection of theoretical calculations of the wave drag of swept wings at zero lift. While the present series of wings have round nose sections, except in special cases the theory for such sections is intractable, and the best that can be done at present is to compare the measured drags with the theoretical drag of wings of the same planform and of a. section for which the theory is tractable, for instance the double wedge.

Much of the theory that exists, and most of the numerical evaluations, are for wings of double wedge section having the maximum thickness at 50% of the chord (m = 0.5). Realising that the agreement between theory for sharp nose (double wedge) sections and. experiment for round nose (aerofoil) sections is not likely to be very good anyhow, the question arises whether the better agreement, if any, obtained when the comparison is made with theory for wings having a double wedge section of the correct maximum thickness position (for example m = 0.31 for RAE.101 section) justifies the extra labour involved in computing such extra curves. In the comparisons that follow, two theoretical curves are given in each instance namely for a wing of the correct planform and having a double wedge section, (a) with the maximum thickness at mid chord - m = 0.5 and (b) with the maximum thickness at the same place as the aerofoil with which comparison is being made - usually m = 0.3 (cf. m = 0.31 for RAE.101).

it should be understood that these theoretical curves are not presented as estimates of the drag of the wings tested; estimates of the drag of wings of round nose section are currently made by applying rough empirical "corrections" to theoretical curves for wings of polygonal section, such as are sham. In some regions the corrections are expected to be large, and the disagreement between the experimental results and the theoretical results added to Figs.21 - 25 should not be interpreted as a measure of the uncertainty of current methods of drag estimation.

In Fig.21, the comparison is made for untapered wings having streamwise tips. The experimental curves are for models of RAE.101 section, with the maximum thickness of 0.31 of the chord. The theoretical curves are for wings of the same A tan $\Lambda_{\frac{1}{2}}$ and of double wedge section, with two values of m ; in this case it is clear that the effect on the drag of a wing of double wedge section of changing from m = 0.5 to the precise value appropriate to the experimental wing is too small to justify the computational labour. Now although it is not to be expected that the experimental curves will exhibit the sharp peaks shown by the theoretical curves, it should be noted that ths relationship between the theoretical and experimental curves is qualitatively consistent in the 3 cases shown in Fig.21. That is to say, comparing each experimental curve with its appropriate theoretical curve, it will be seen that at given intervals of $A\sqrt{M^2-1}$ less then that corresponding to the peak in the theoretical drag curve $[\Delta(A\sqrt{M^2-1})]$, the ratio between theoretical and experimental drag is consistent, e.g. about $1\frac{1}{2}$ at the value of $A\sqrt{M^2-1}$ corresponding to the peak, 1 at about $\Delta(A\sqrt{M^2-1}) = -\frac{1}{2}$ and about $\frac{1}{2}$ at $A(A\sqrt{M^2-1}) = -2$.

The results for two swept untapered wings with cut-off tips shown in Flg.22, have already been introduced. The curious result for Model 4 has already been commented on; it must at this stage bc assumed real, end certainly indicates that the theoretical refinement of moving the maximum thickness position is not justified.

In Fig.23 we have compared the two delta wings. According to the similarity laws the two Models 6 and 7 should have the same drag when plotted in this manner, and the poor agreement is a little disappointing. The effect on the theoretical curve of varying the value of m is large, and it seems in this instance that the change is worth while.

---

* Estimated by interpolation from the curves of Ref.4.

In Fig.24 the results for the 4 cropped delta Models 8, 9, 10 and 11 have been collapsed according to the similarity laws; here, where we have 3 different sections and 4 different thicknesses, the collapse is quite good. Again, the variation of m has a profound effect on the drag of the double wedge wing, and, at least when the wing is "subsonic', better agreement with experiment is achieved by considering the double wedge wing hating the same maximum thickness position.

Fig.25 is comparable with Fig.23, in that Models 12 and 13a should, according to this method of plotting, have identical drag curves. The agreement between the two curves is very satisfactory. On the theoretical side it is seen that the two experimental results in Fig.25 bear the same qualitative relationship to the two theoretical curves, as does the experimental result for Model 7 in Fig.23 when it is remembered that a value of $A\sqrt{M^2-1}$ of about unity in Fig.23, corresponds, as far as the geometry of the flowabout the wing is concerned, to a value of about 3 in Fig.25.

6 Concluding Remarks

The results presented hen? are a rather random selection, and in themselves do not justify any weeping conclusions. *Par* more experimental results and comparisons with theory are required before any unifying picture can be drawn. In addition it would be desirable to have comparisons with the theoretical results for wings of the correct section. Such theoretical results are not available and the comparisons made here have all been between experiments on wings of "smooth" profile aerofoil section, and theory for wings of "kinked" profile double wedge section, and these kinks lead to the characteristic peaks in the drag curves, many of which would not occur in the theory for wings of smooth profile. Good agreement in the comparisons shown here would therefore not be expected. But from these results three preliminary conclusions are offered.

(a) At supersonic speeds, the wave drag of a given wing varies as the square of the thickness ratio;

(b) the supersonic similarity law allows the drag of 'similar' wings to be compared; and

(c) there is some hope that the drag of round-nose section wings can be estimated from theoretical calculations of the drag of wings of double wedge section.

The next step in this work is to compare these results with other published measurements of the drag of swept wings.

NOTATION

A = nett aspect ratio

$= \dfrac{(\text{twice exposed semi-span})^2}{S_W}$

$\bar{c}$ = mean chord - feet

$= \dfrac{S_W}{\text{twice exposed semi-span}}$

C_{D_B} = drag coefficient based on S_B

C_{D_f} = wing friction drag coefficient based on S_W

C_{D_o} = wing profile drag coefficient based on S_W

C_{D_W} = wing wave drag coefficient based on S_W

$= C_{D_o} - C_{D_f}$

L = leading edge of root chord aft of body nose - inches

M = Mach Number

m_o = position of maximum thickness aft of nose

S_B = body frontal area

= 0.222 square feet

S_W = exposed wing area - square feet

λ = taper ratio

$= \dfrac{\text{tip chord}}{\text{root chord}}$

Λ_o = sweep of leading edge

$\Lambda_{\frac{1}{2}}$ = sweep of half chord line

Λ_1 = sweep of trailing edge

$\sigma = \dfrac{\tan \Lambda_1}{\tan \Lambda_o}$

τ = ratio $\dfrac{\text{thickness}}{\text{chord}}$, streamwise

REFERENCES

No.	Author	Title, etc.
1	Lawrence Swan and Warren	Development of a transonic research technique using ground-launched rocket-boosted models: Part II - Drag measurements. A.R.C. 14167. February, 1951.
2	Cope	The turbulent boundary layer in compressible flow. R & M.2840. November, 1943.
3	Thompson	The supersonic pressure drag of a swept wing with a cranked maximum thickness line. C.P.61. June, 1950.
4	Lawrence	Charts of the wave drag of wings at zero lift. R.A.E. Technical Note No. Aero.2139. C.P.116. November, 1952.

11t.2078. CP145.K3. - Printed in Great Britain.

TABLE I. DETAILS OF TEST MODELS.

MODEL	PLANFORM	Nº OF WINGS	SECTION	τ	Λ_0	$\Lambda_{1/2}$	σ	λ	A	A tan $\Lambda_{1/2}$	S_B/S_W	L ③	$\bar{c}$
1	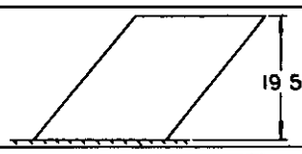	2	RAE 101	0·061	40	40	1·0	1·0	1·88	1·58	·0395	51·0	1·73
2	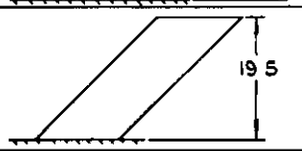	2	RAE 101	0·06	45	45	1·0	1·0	3·0	3·00	·0631	55·0	1·08
3	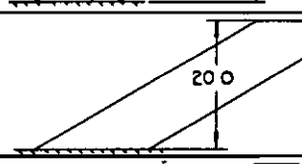	2	RAE 101	0·06	60	60	1·0	1·0	2·31	3·96	·0457	46·3	1·78
4a 4b 5a 5b	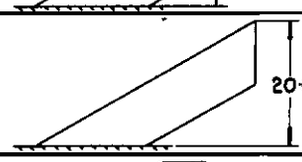	2 3 2 3	RAE 101 RAE 104	0·06 0·06	60	—	[UNTAPERED INBOARD]		3·0 (e)	—	·0609 ·0407 ·0609 ·0407	55·0 55·0	1·10
6	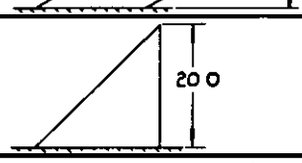	2	RAE 101	0·06	45	26·6	0	0	4·00	2·00	·0631	53·0	0·83
7	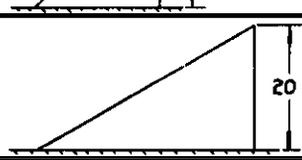	2	RAE 101	0·06	60	40·9	0	0	2·31	2·00	·0463	46·0	1·44
8	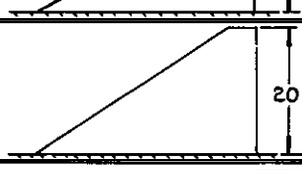	2	NACA 0010	0·10	53·3	33·9	0	0·128	2·31	1·55	·0357	51·2	1·64
9a 9b	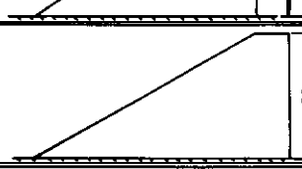	2 3	RAE 101	0·06	60	40·9	0	0·143	1·73	1·50	·0346 ·0231	45·1 48·0	1·92
10 11	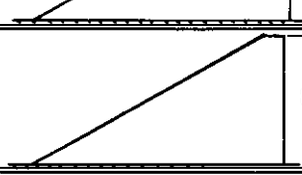	2 2	①	0·04 ② 0·04-·09	60	4·to 9	0	0·084	1·9·6	1·70	·0355	40·0	1·78
12	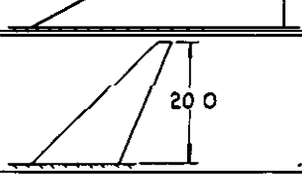	2	RAE 101	0·06	45	31·5 1	0·438	0·143	5·3·3	3·83	·1068	64·0	0·63
13a 13b 14	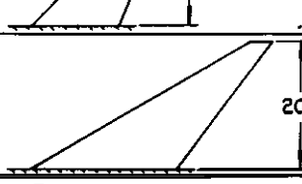	2 3 3	RAE 101	0·06 0·06 0·10	60	51·2	0·438	0·143	3·08	3·83	·0610 ·0407 ·0407	49·8 53·8 53·8	1·10

NOTES ① SPECIAL SECTION - τ MAX AT 0·3C, THICKER FORE & AFT THAN RAE 101
② THICKNESS VARIES SPANWISE - SEE FIG 4
③ SEE FIG 1

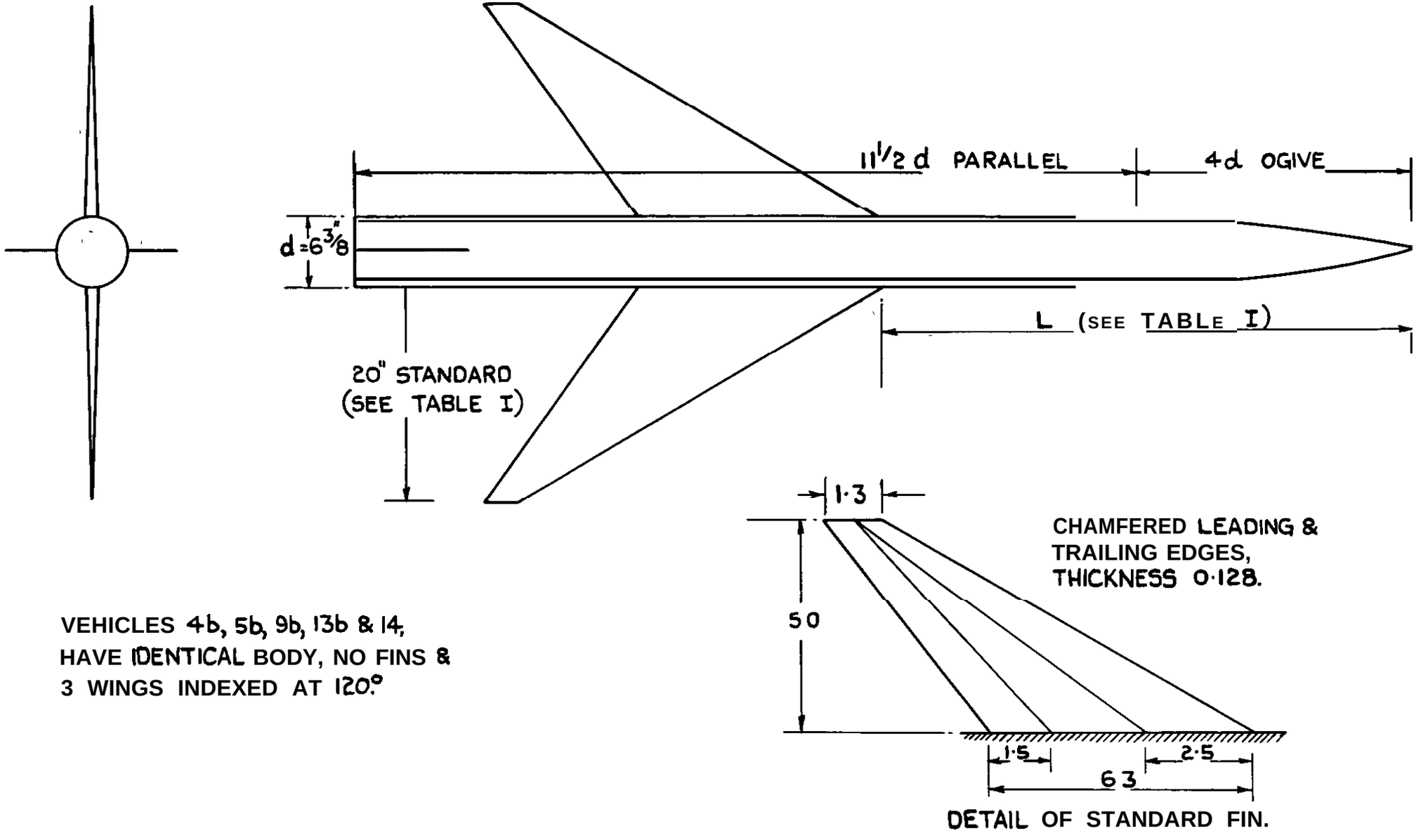

VEHICLES 4b, 5b, 9b, 13b & 14,
HAVE IDENTICAL BODY, NO FINS &
3 WINGS INDEXED AT 120°

FIG. 1. G.A. OF 2 WING TEST VEHICLE (NOMINAL DIMENSIONS IN INCHES)

FIG.1.

FIG.2

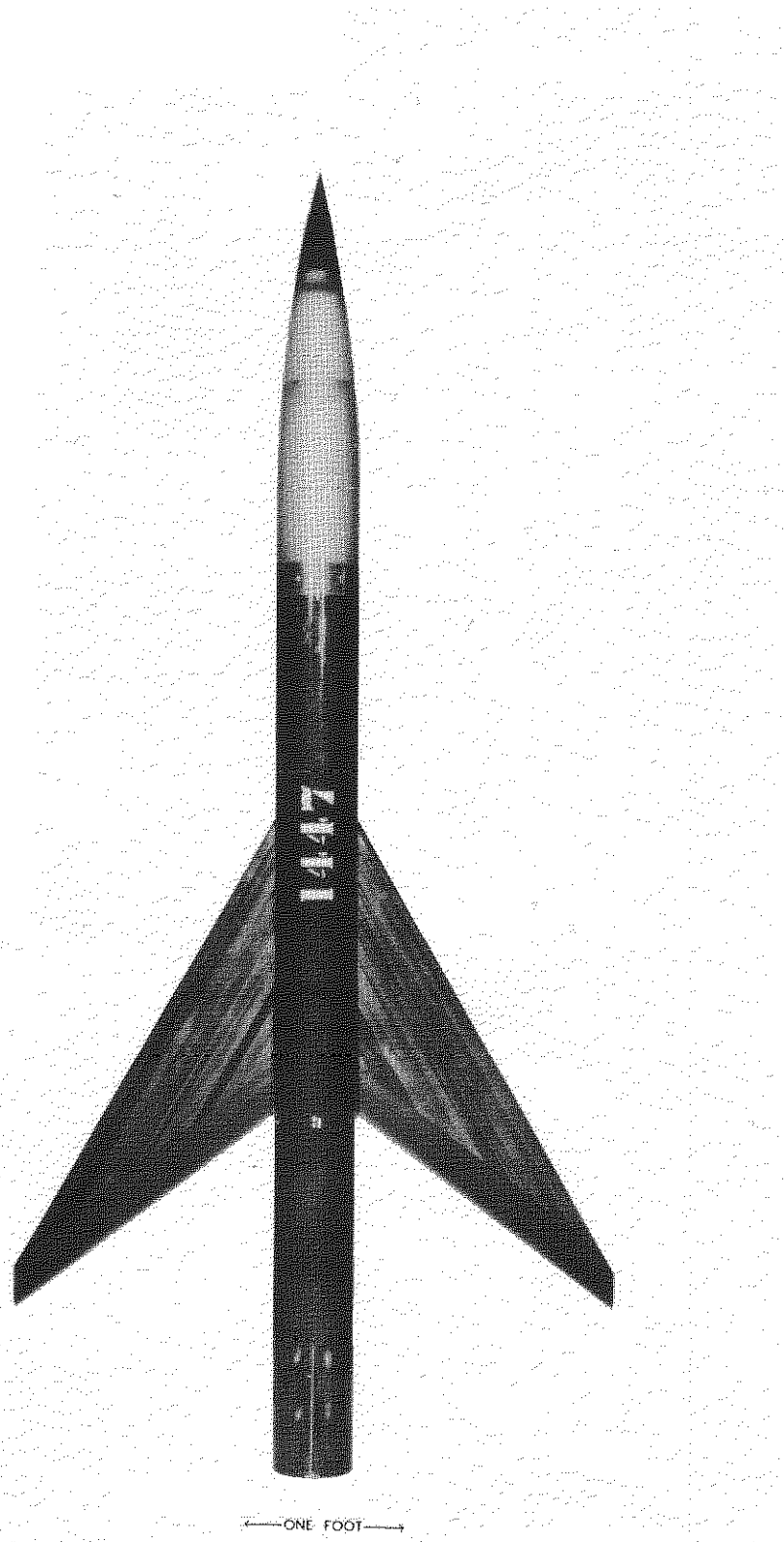

FIG. 2. TYPICAL TEST VEHICLE

MODEL 13a

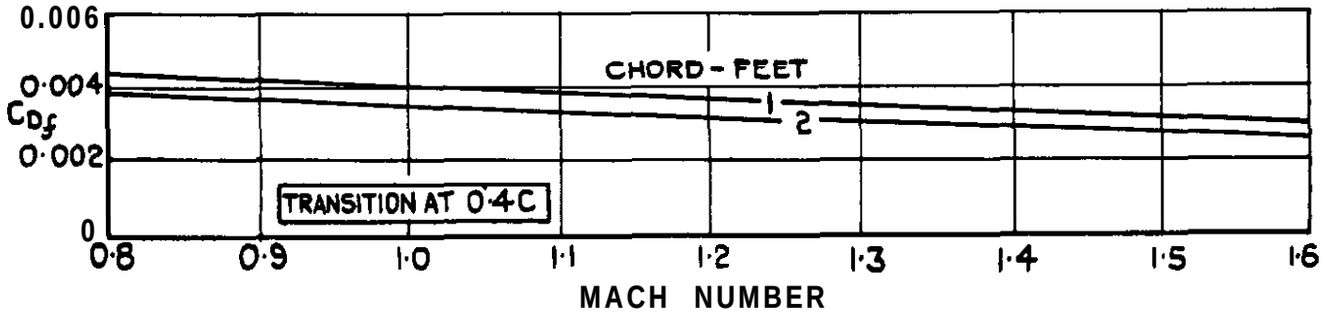

FIG. 3. WING FRICTION DRAG COEFFICIENT.

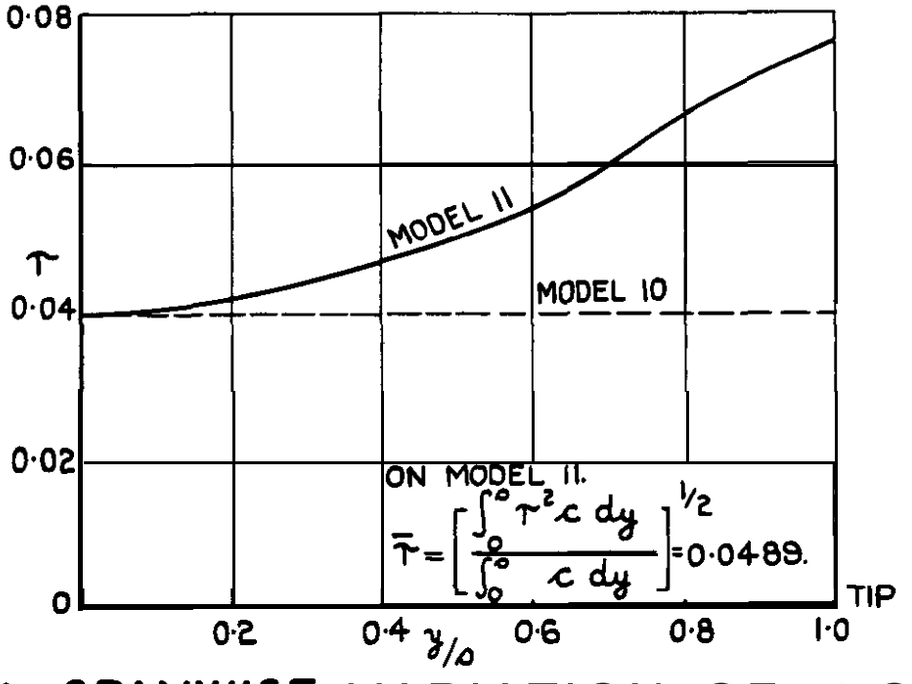

FIG. 4. SPANWISE VARIATION OF τ ON MODELS IO & II.

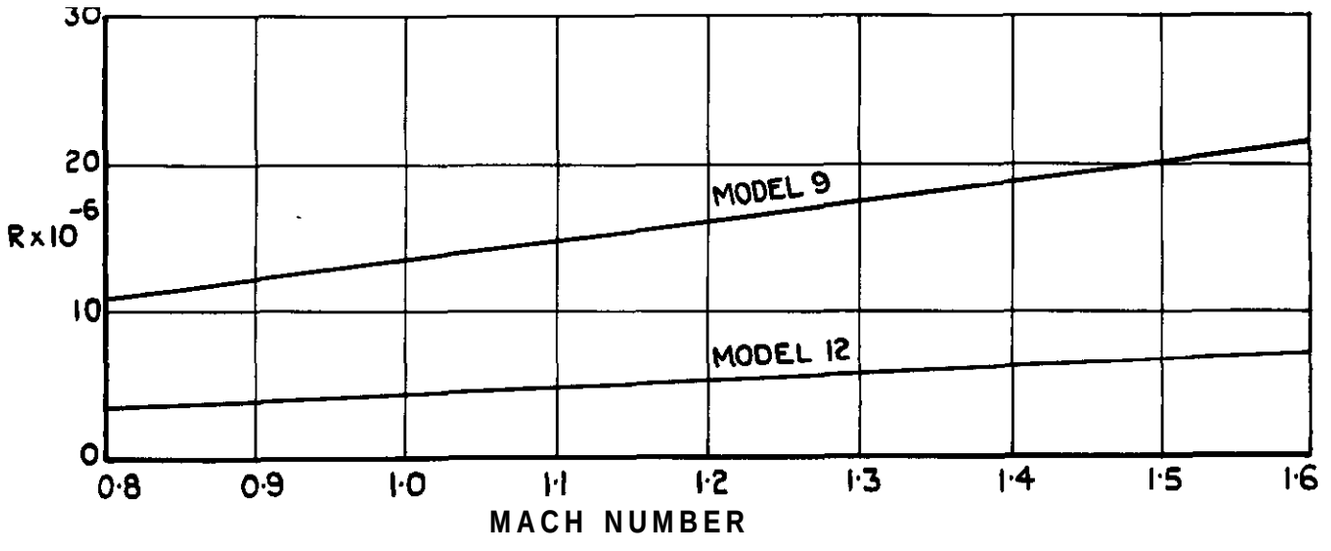

FIG. 5. VARIATION OF REYNOLDS NUMBER FOR LARGEST AND SMALLEST MODELS,

FIG. 6 (a & b)

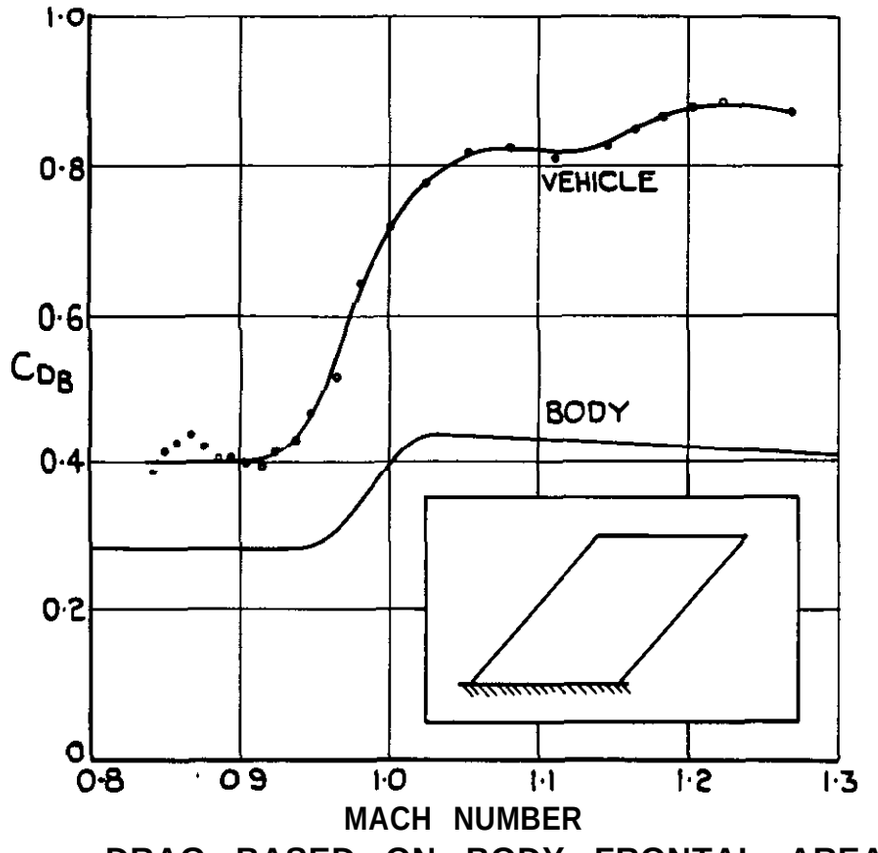

(a) DRAG BASED ON BODY FRONTAL AREA.

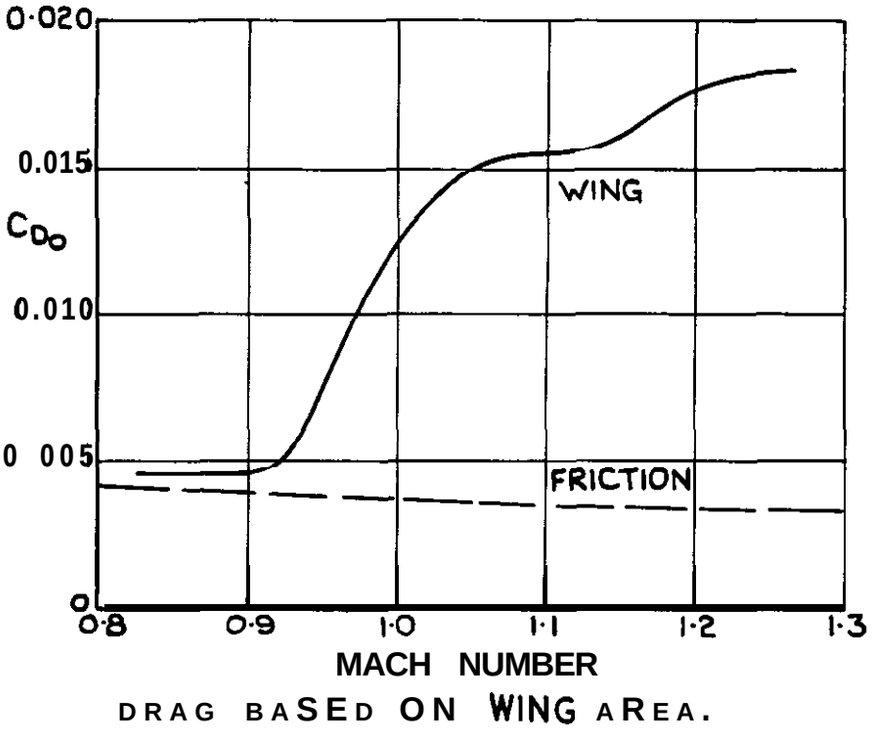

(b) DRAG BASED ON WING AREA.

FIG. 6 (a & b) ORAG OF MODEL I.

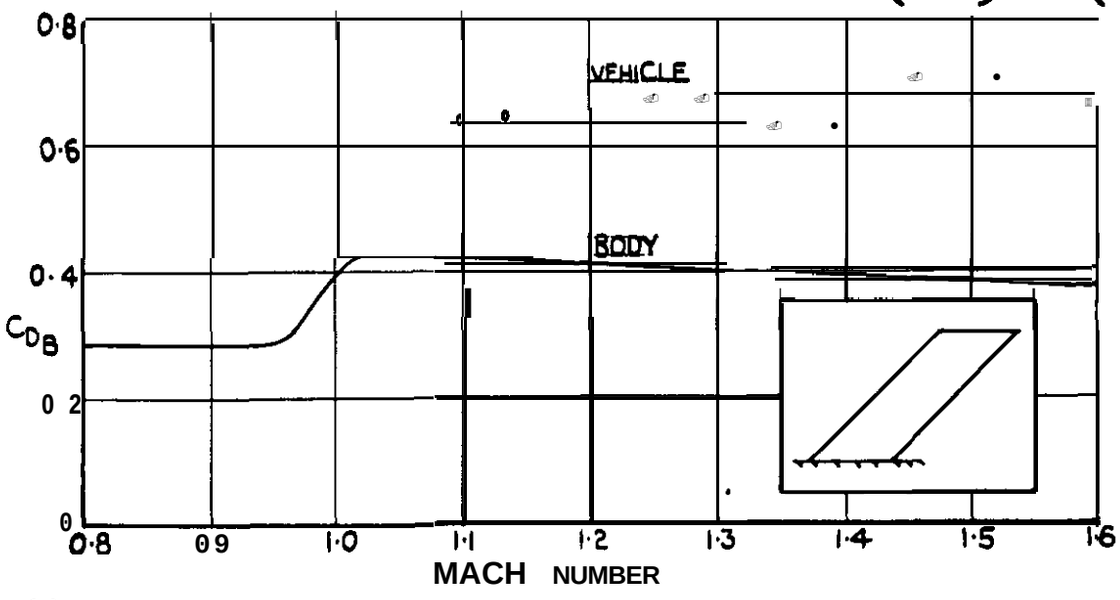

(a) DRAG BASED ON BODY FRONTAL AREA.

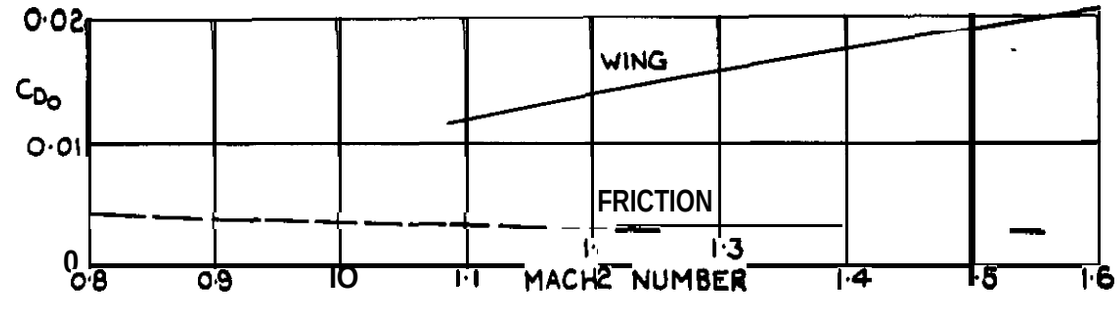

(b) DRAG BASED ON WING AREA.

FIG. 7 (a & b) DRAG OF MODEL 2.

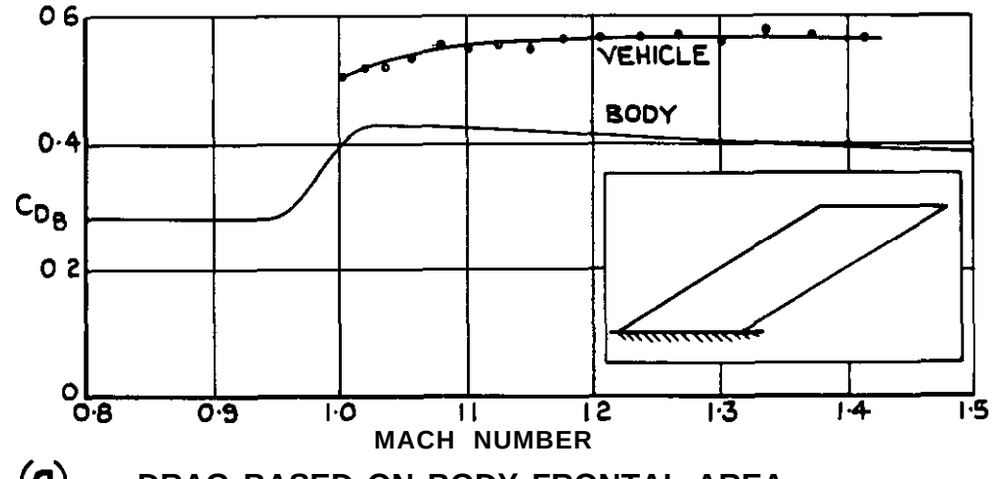

(a) DRAG BASED ON BODY FRONTAL AREA

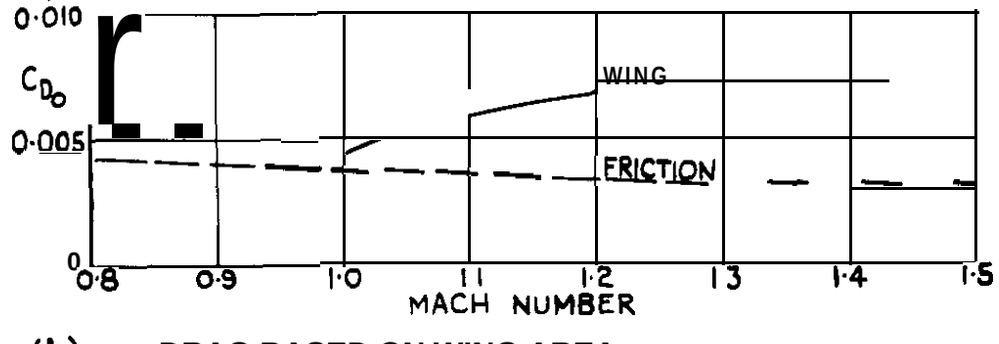

(b) DRAG BASED ON WING AREA

FIG. 8. (a & b) DRAG OF MODEL 3

FIG. 9.(a & b)

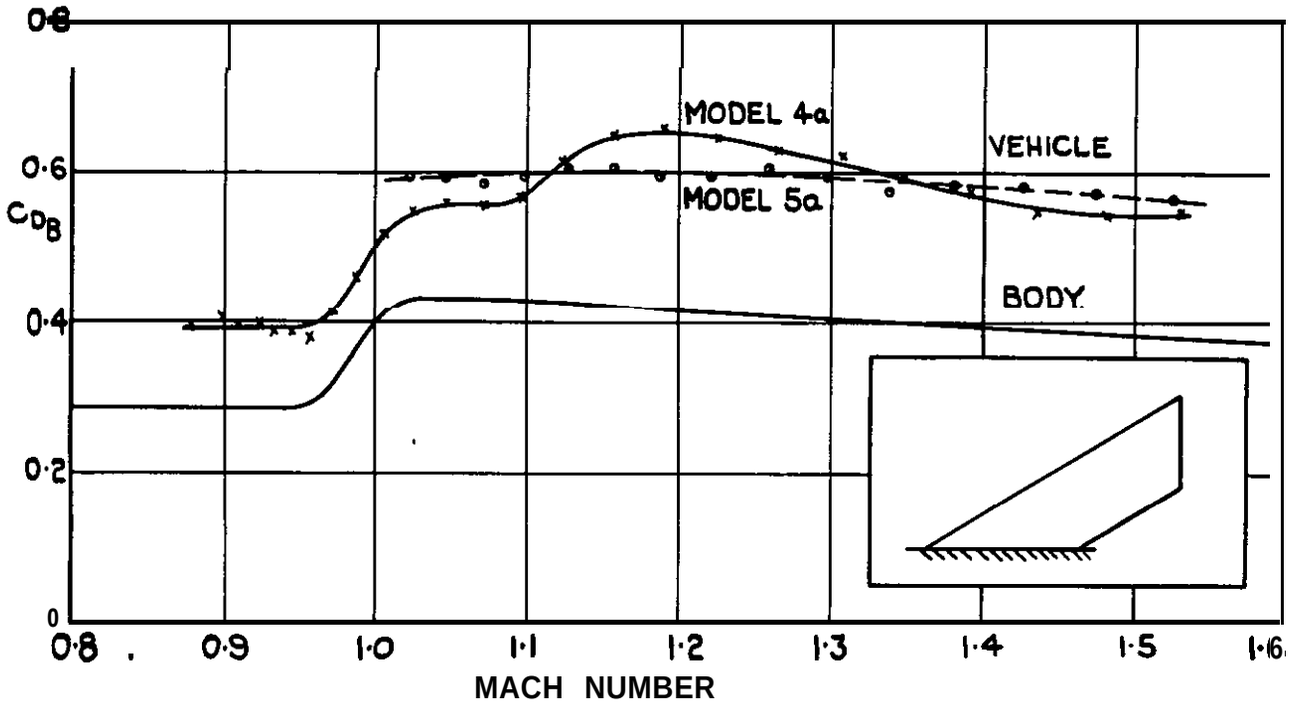

(a) DRAG BASED ON BODY FRONTAL AREA.

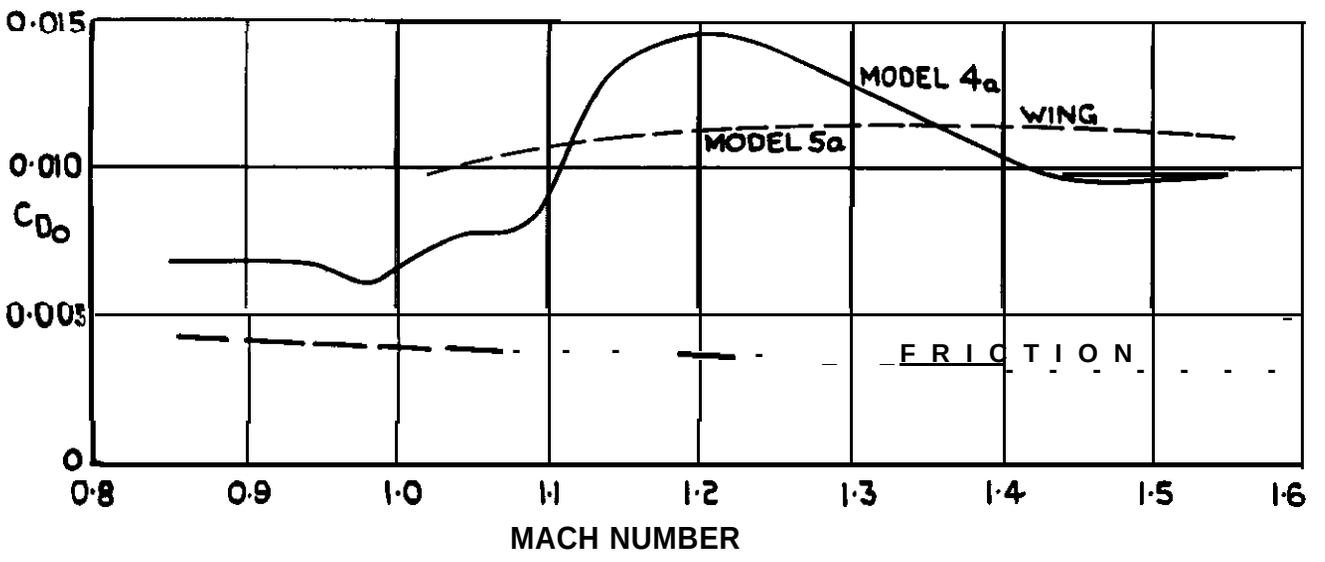

(b) DRAG BASED ON WING AREA.

FIG. 9 (a & b) DRAG OF MODELS 4a & 5 a.

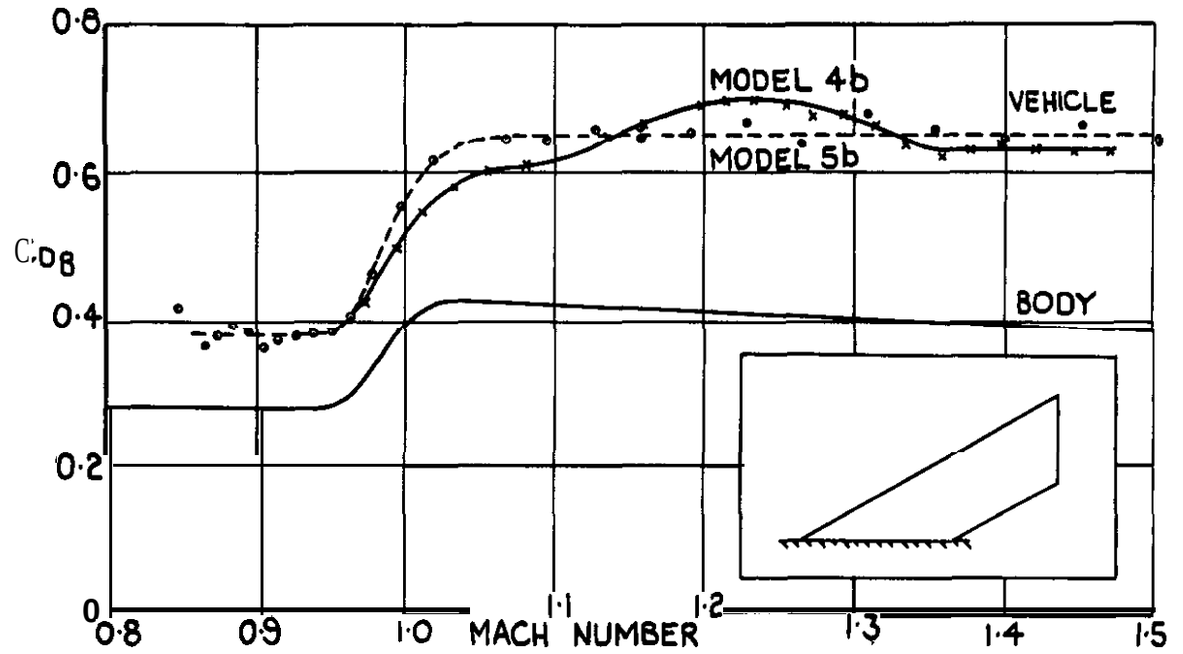

(c) DRAG BASED ON BODY FRONTAL AREA.

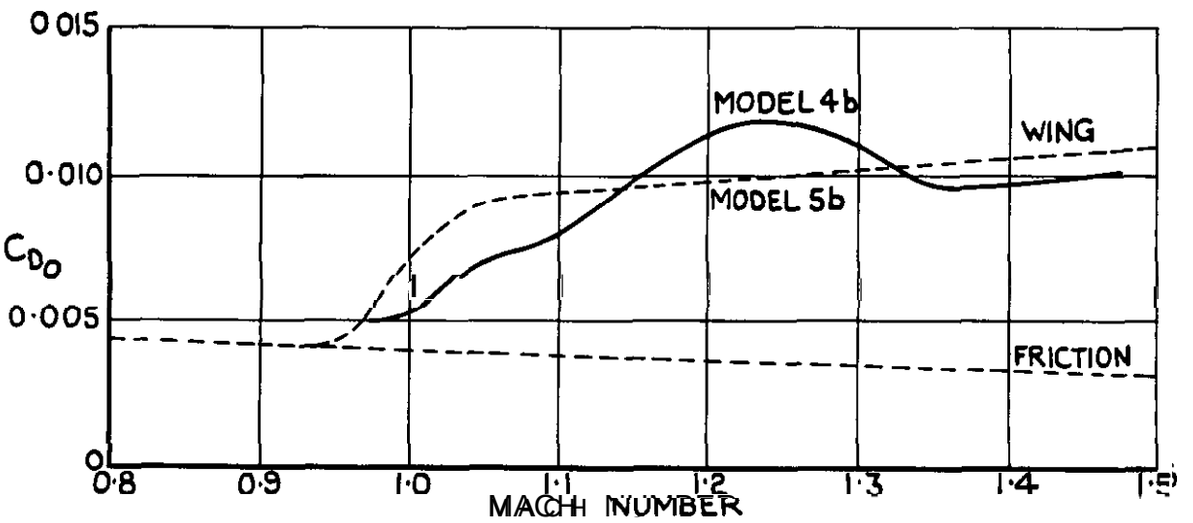

(d) DRAG BASED ON WING AREA.

FIG.9.(c & d) DRAG OF MODELS 4b & 5b.

FIG.10(a&b)

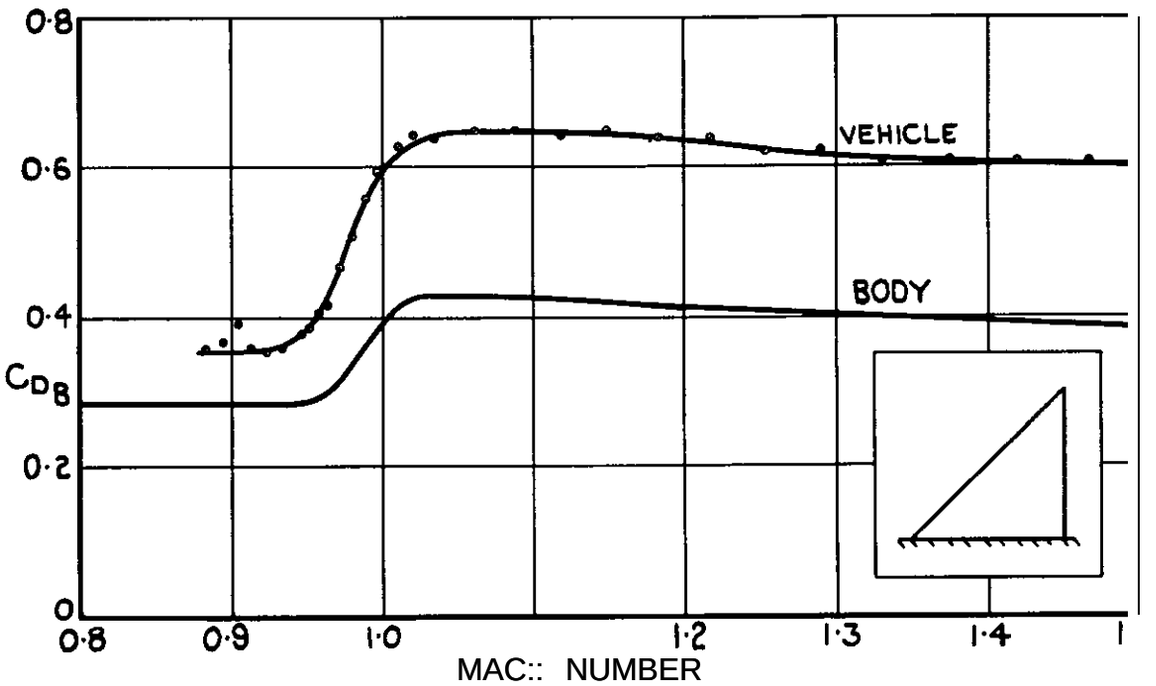

(a) DRAG BASED ON BODY FRONTAL AREA.

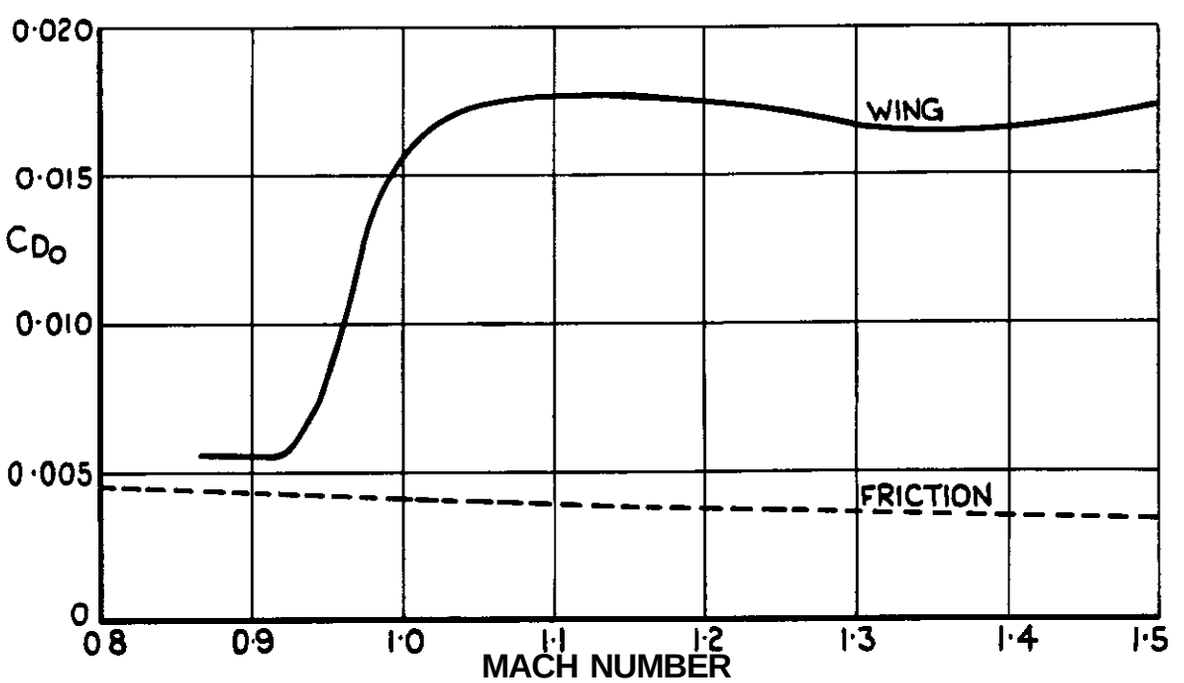

(b) DRAG BASED ON WING AREA.

FIG.10(a&b) DRAG OF MODEL 6.

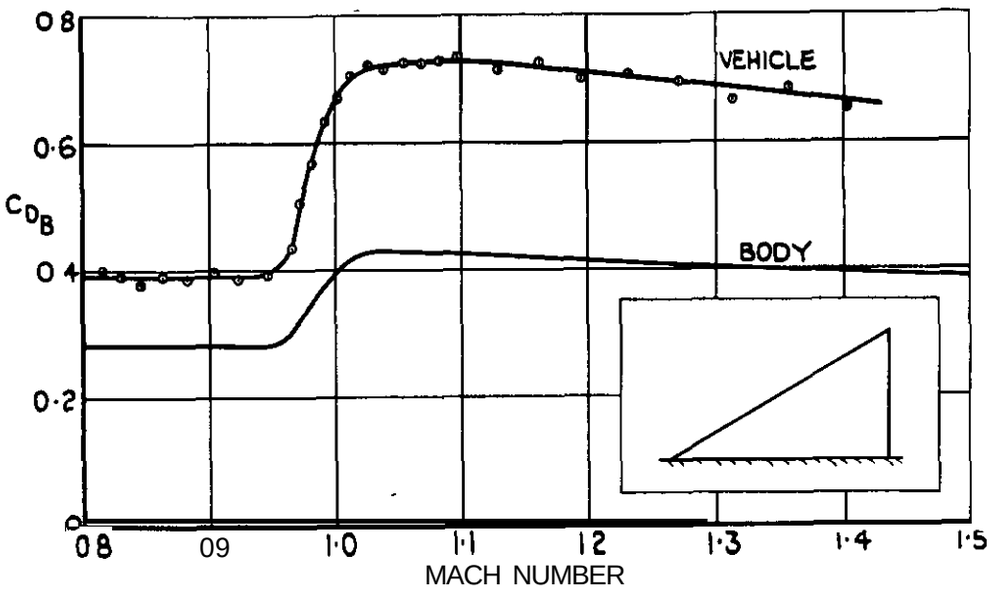

(a) DRAG BASED ON BODY FRONTAL AREA.

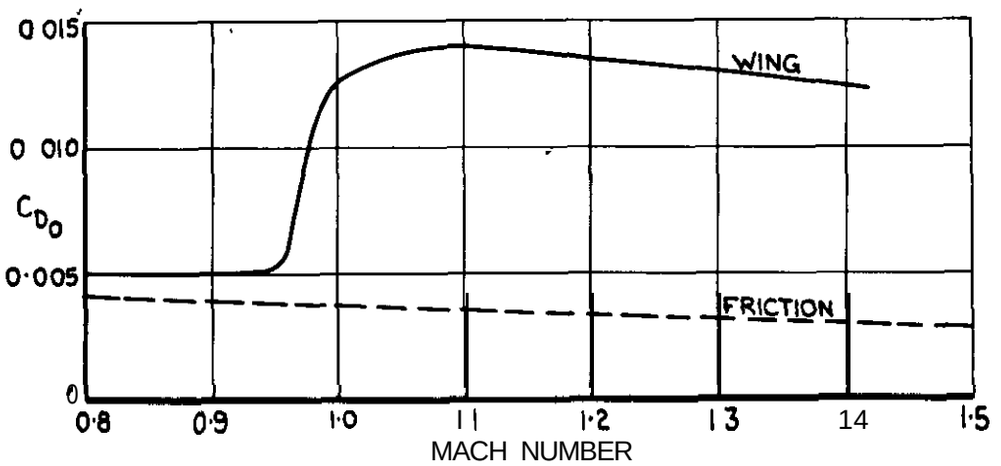

(b) DRAG BASED ON WING AREA.

FIG. 11(a&b) DRAG OF MODEL 7.

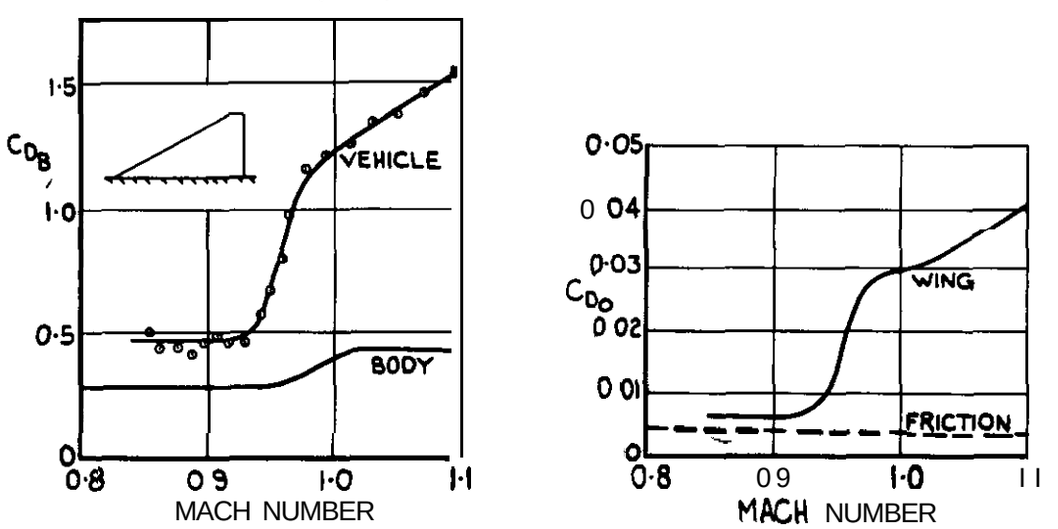

(a) DRAG BASED ON BODY FRONTAL AREA **(b)** DRAG BASED ON WING AREA

FIG.12(a&b) DRAG OF MODEL 8.

FIG. 13. (a & b)

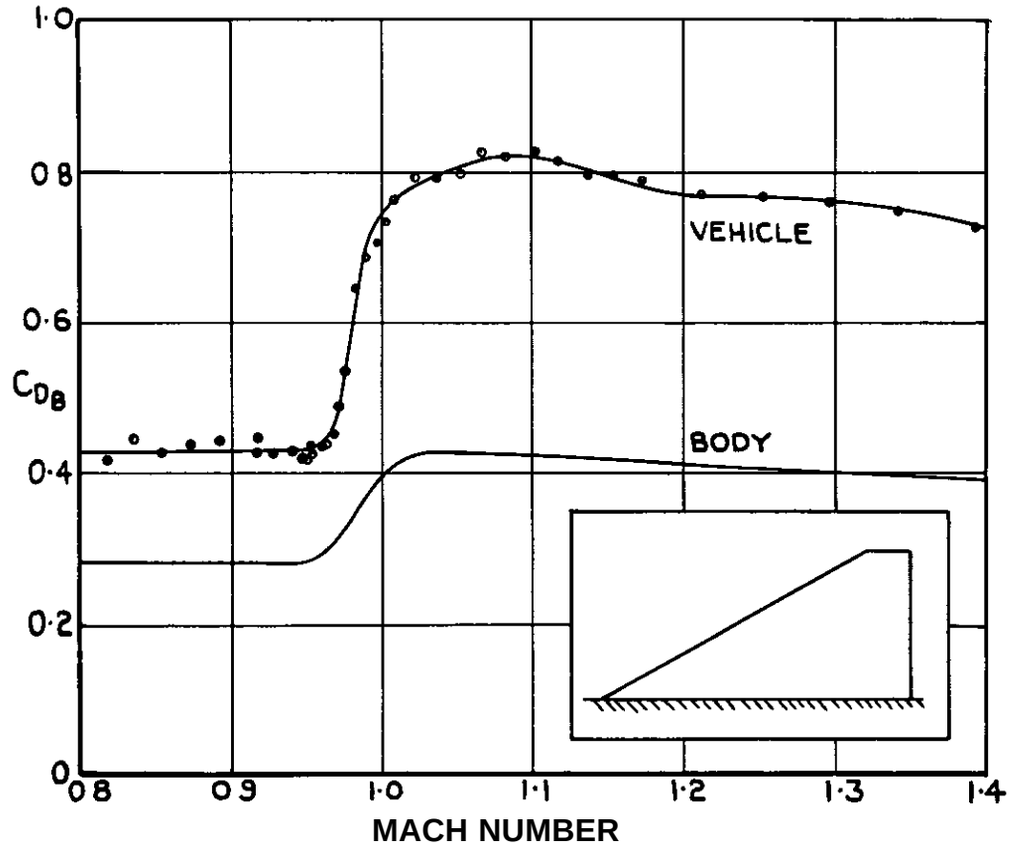

(a) DRAG BASED ON BODY FRONTAL AREA.

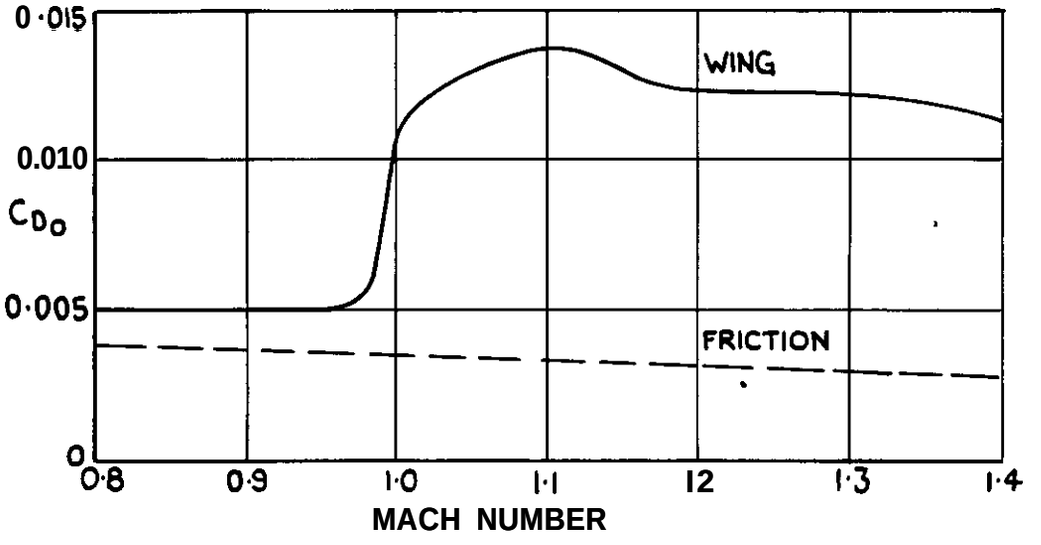

(b) DRAG BASED ON WING AREA.

FIG. 13 (a & b) DRAG OF MODEL 9 a

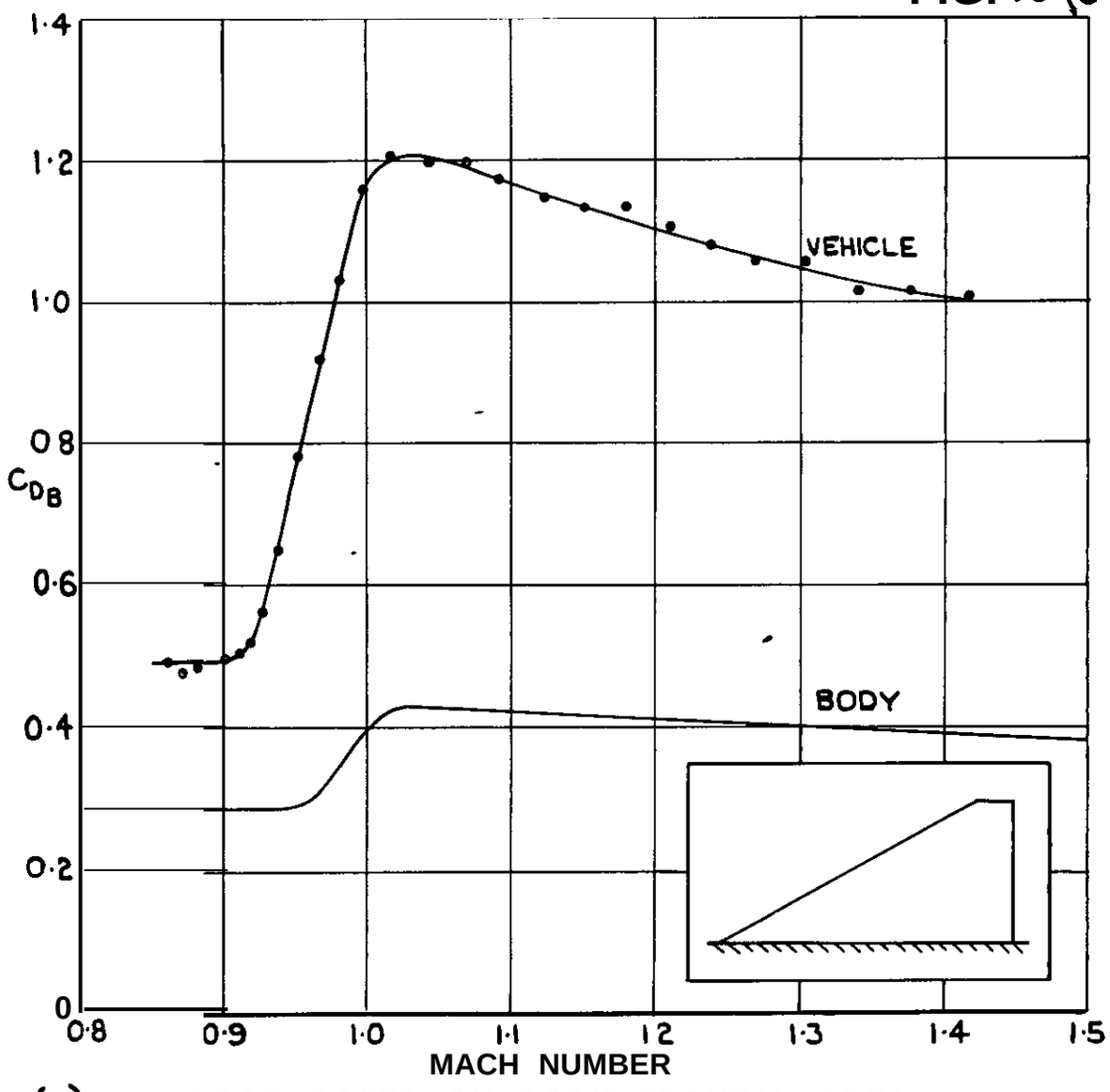

(c) DRAG BASED ON BODY FRONTAL AREA,

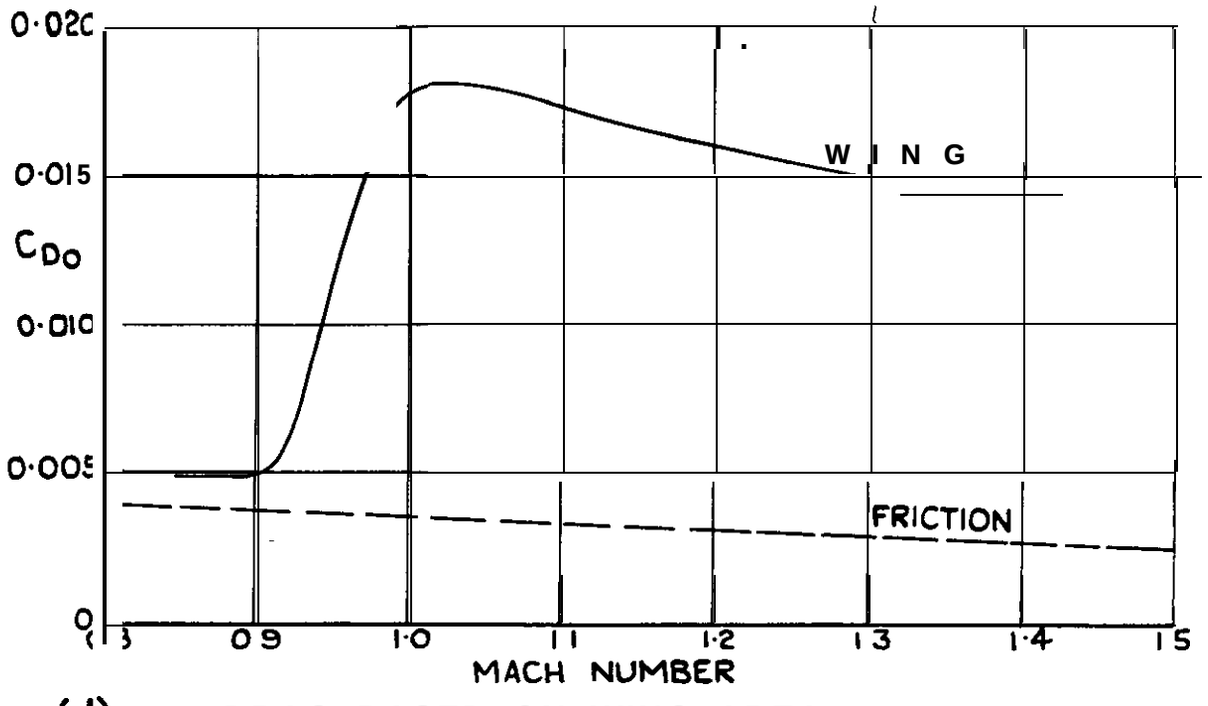

(d) DRAG BASED ON WING AREA.

FIG. 13 (c ad) DRAG OF MODEL 9 b

FIG.14(a&b)

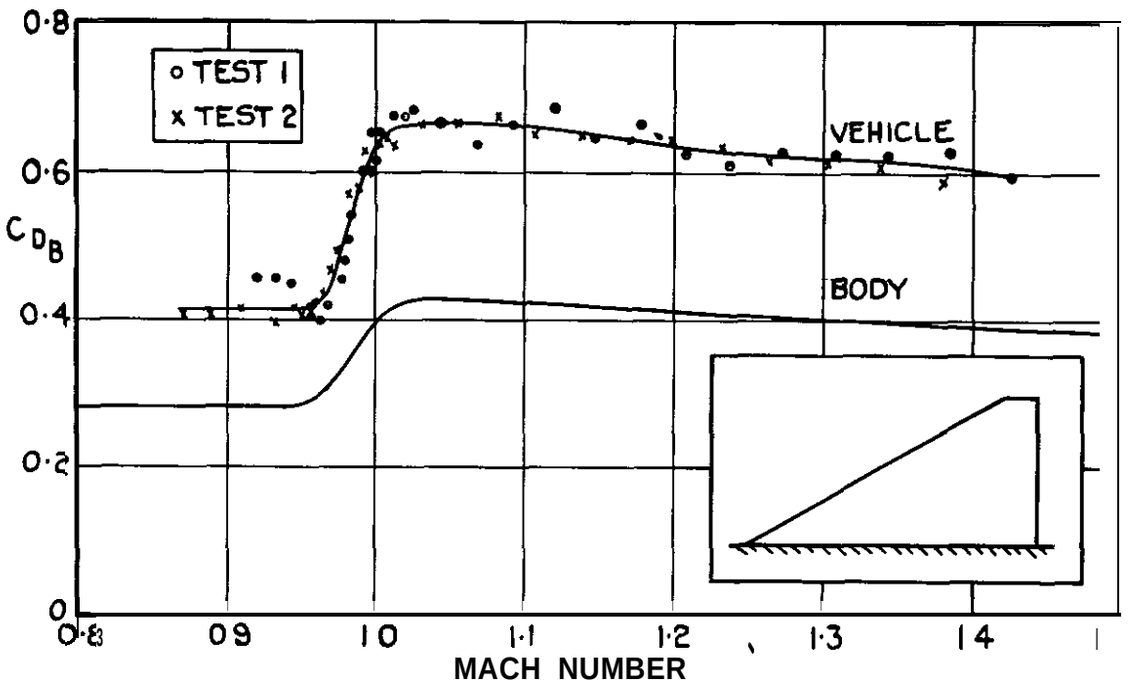

(a) DRAG BASED ON BODY FRONTAL AREA.

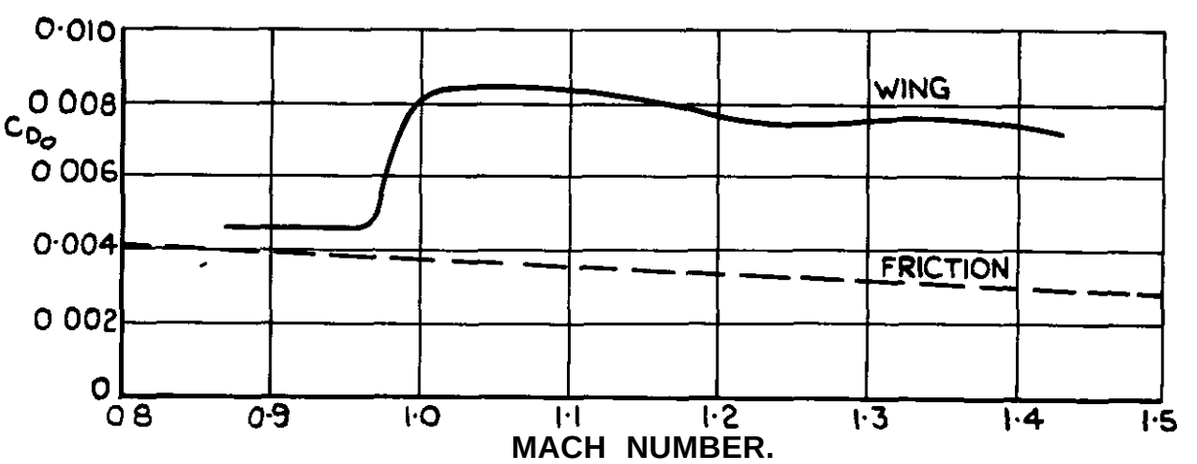

(b) DRAG BASED ON WING AREA.

FIG.14(a&b) DRAG OF MODEL IO.

FIG.15 (a & b)

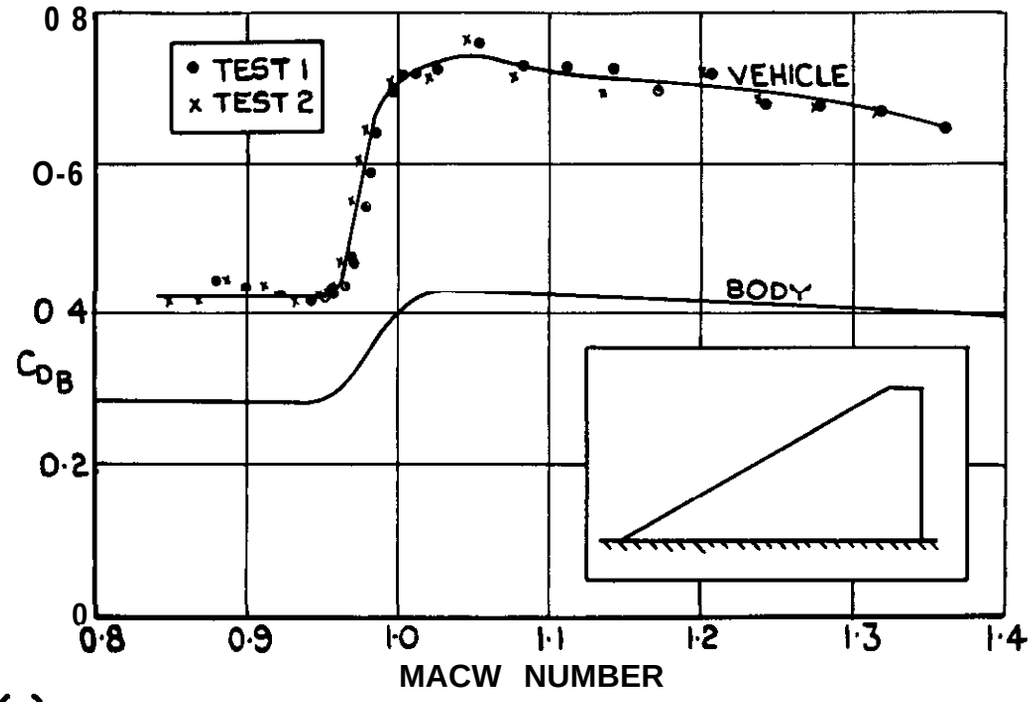

(a) DRAG BASED ON BODY FRONTAL AREA

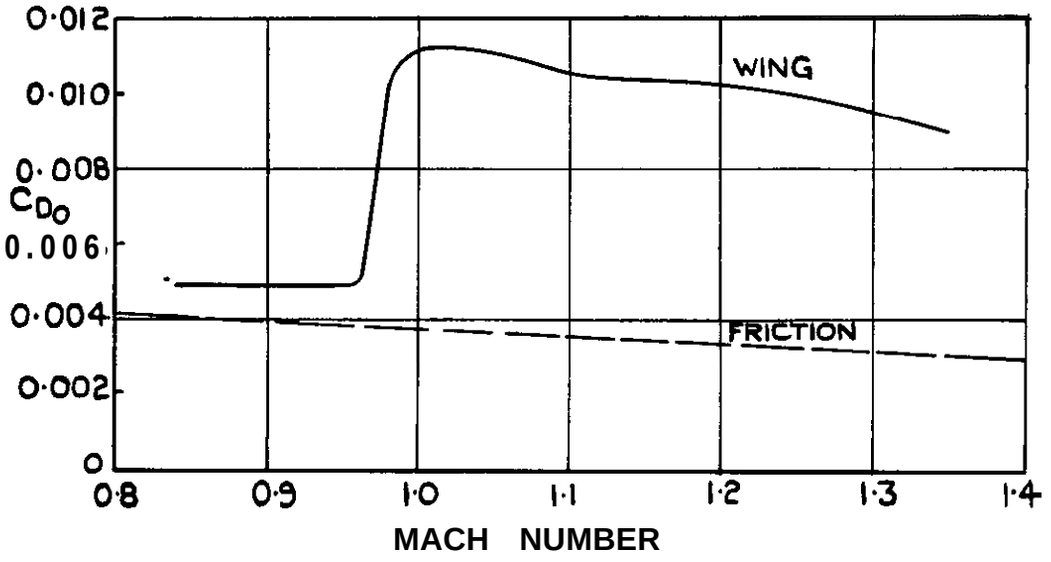

(b) DRAG BASED ON WING AREA.

FIG. 15 (a a b) DRAG OF MODEL II .

FIG.16 (a&b)

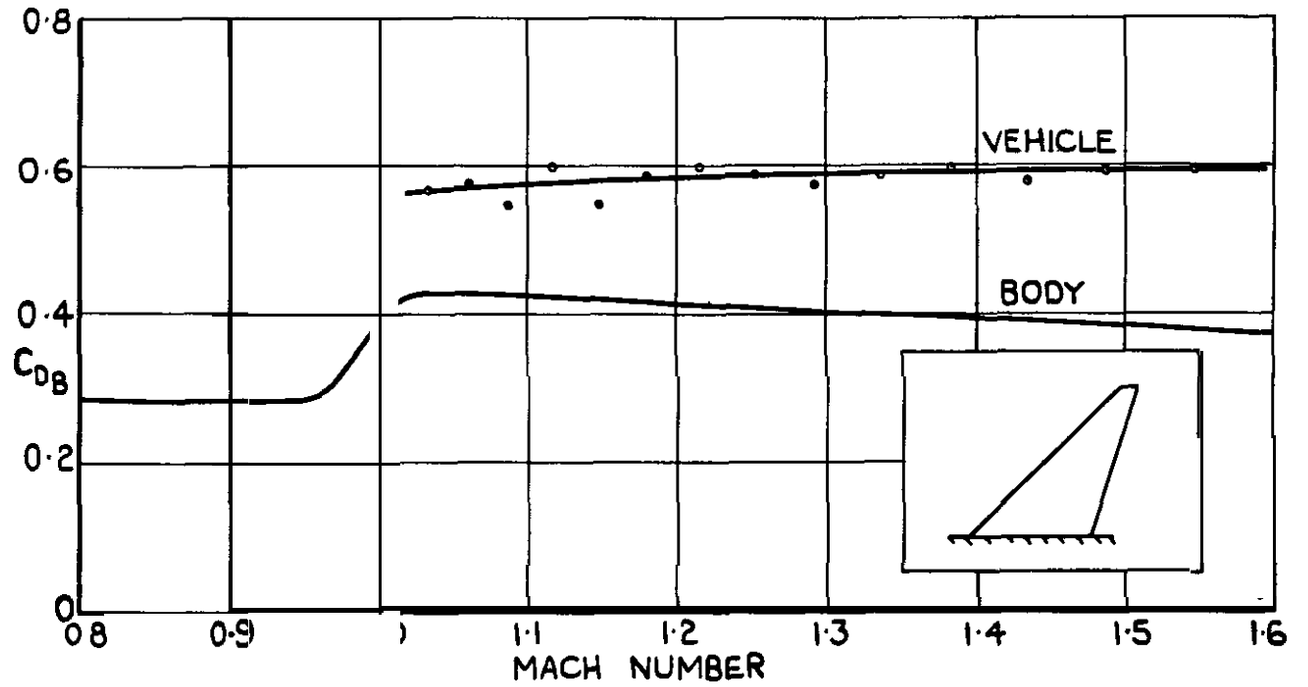

(a) DRAG BASED ON BODY FRONTAL AREA.

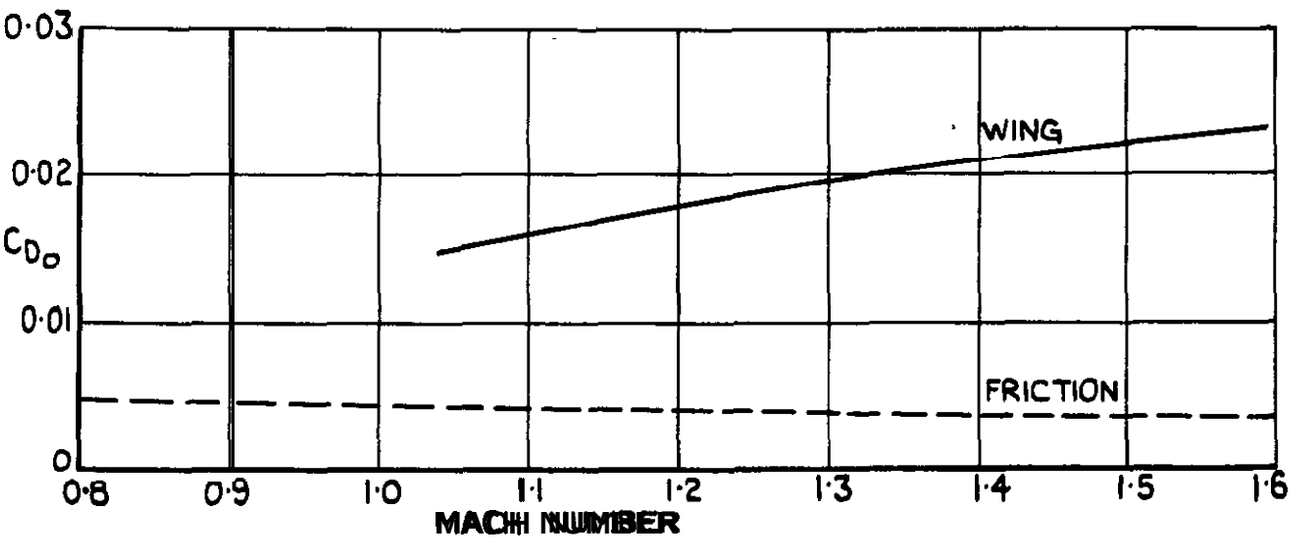

(b) DRAG BASED ON WING AREA.

FIG.16(a & b) DRAG OF MODEL 12.

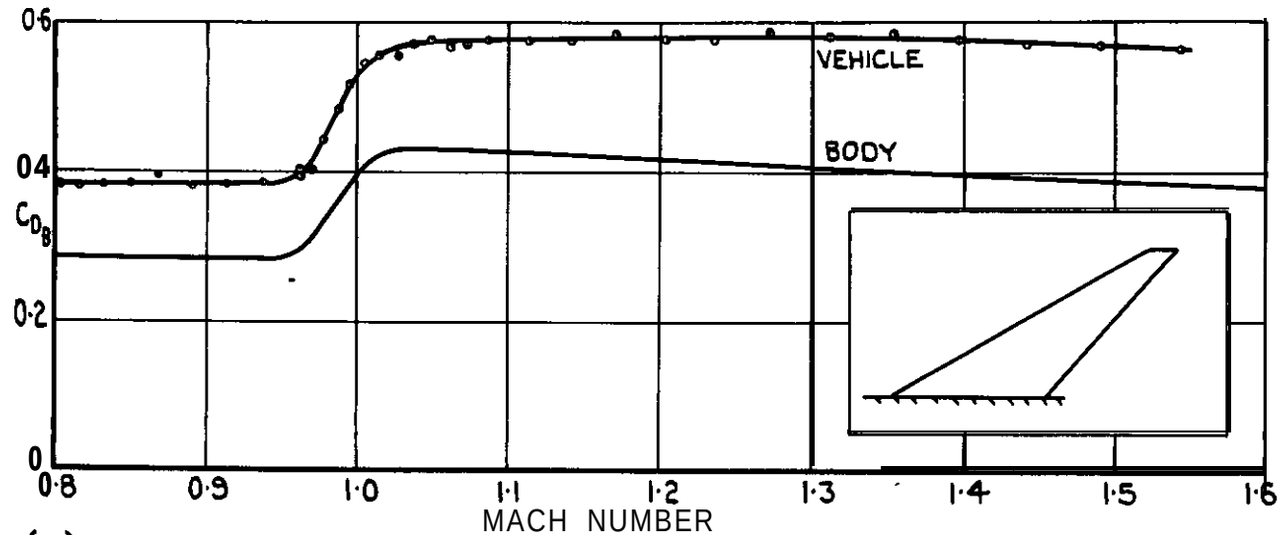

(a) DRAG BASED ON BODY FRONTAL AREA,

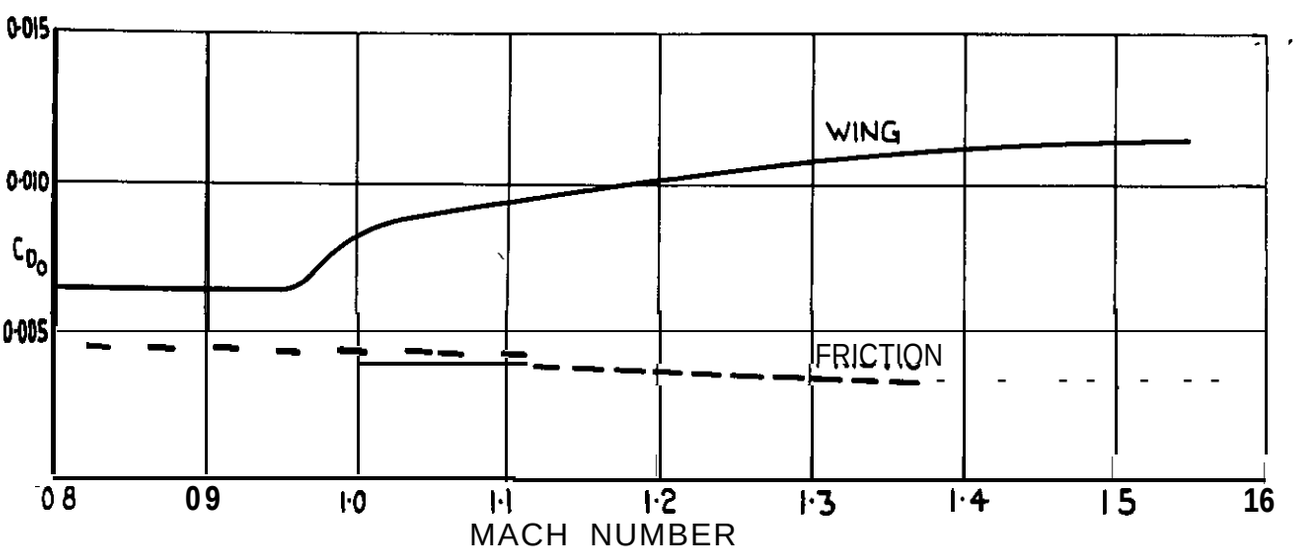

(b) DRAG BASED ON WING AREA.

FIG. 17(a & b) DRAG OF MODEL 13a.

FIG.17(c&d)

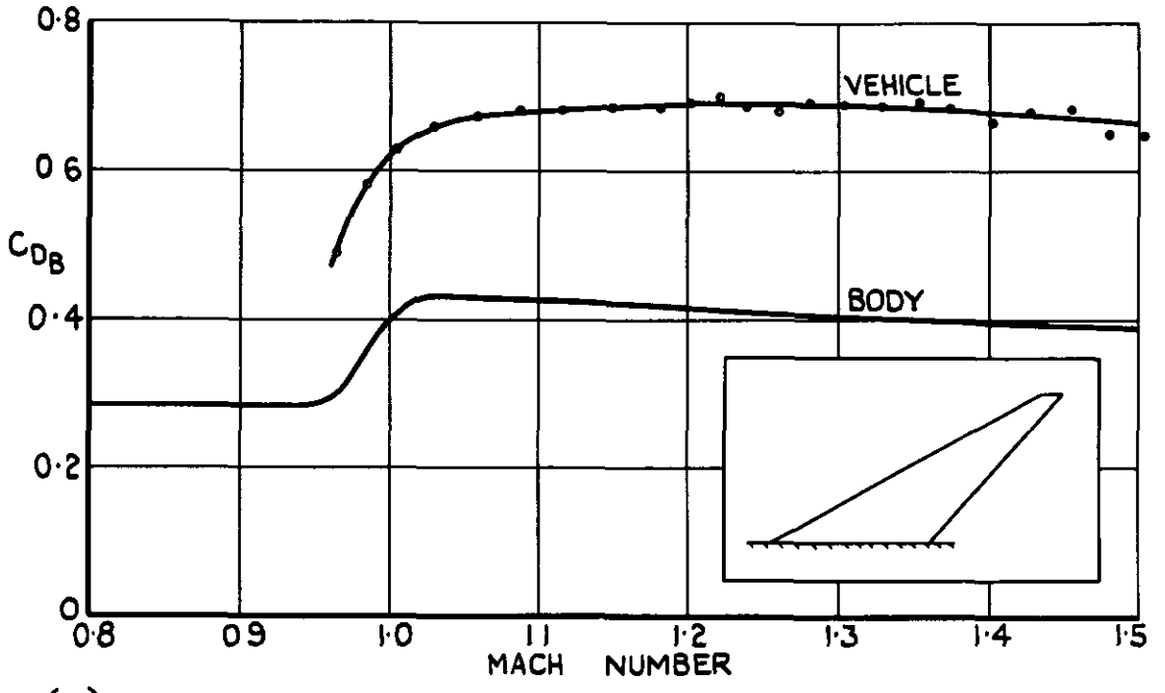

(c) DRAG BASED ON BODY FRONTAL AREA.

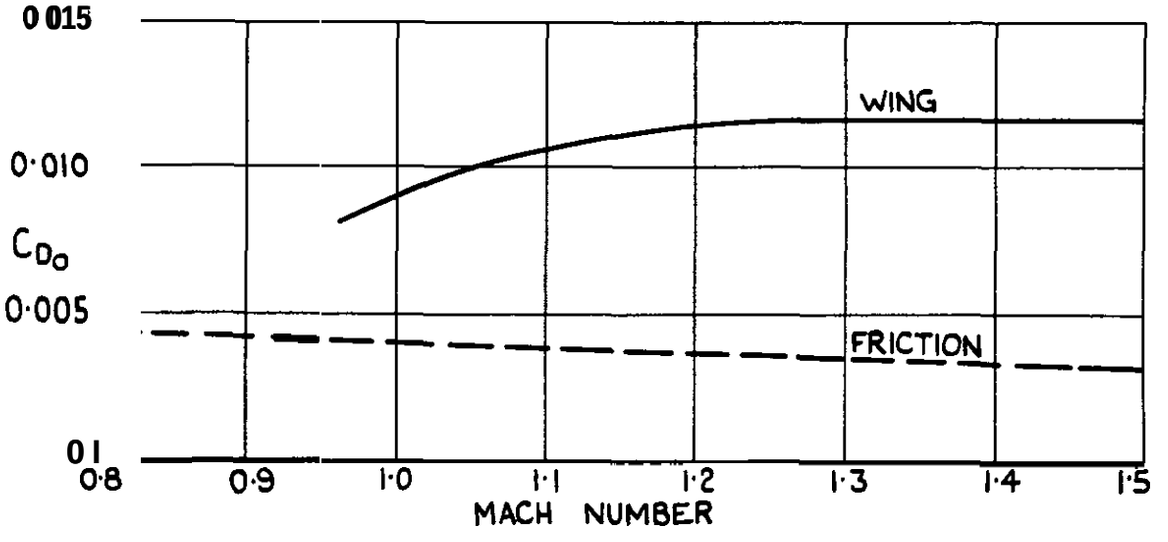

(d) DRAG BASED ON WING AREA.

FIG.17(c&d) DRAG OF MODEL 13b.

FIG.18(a & b)

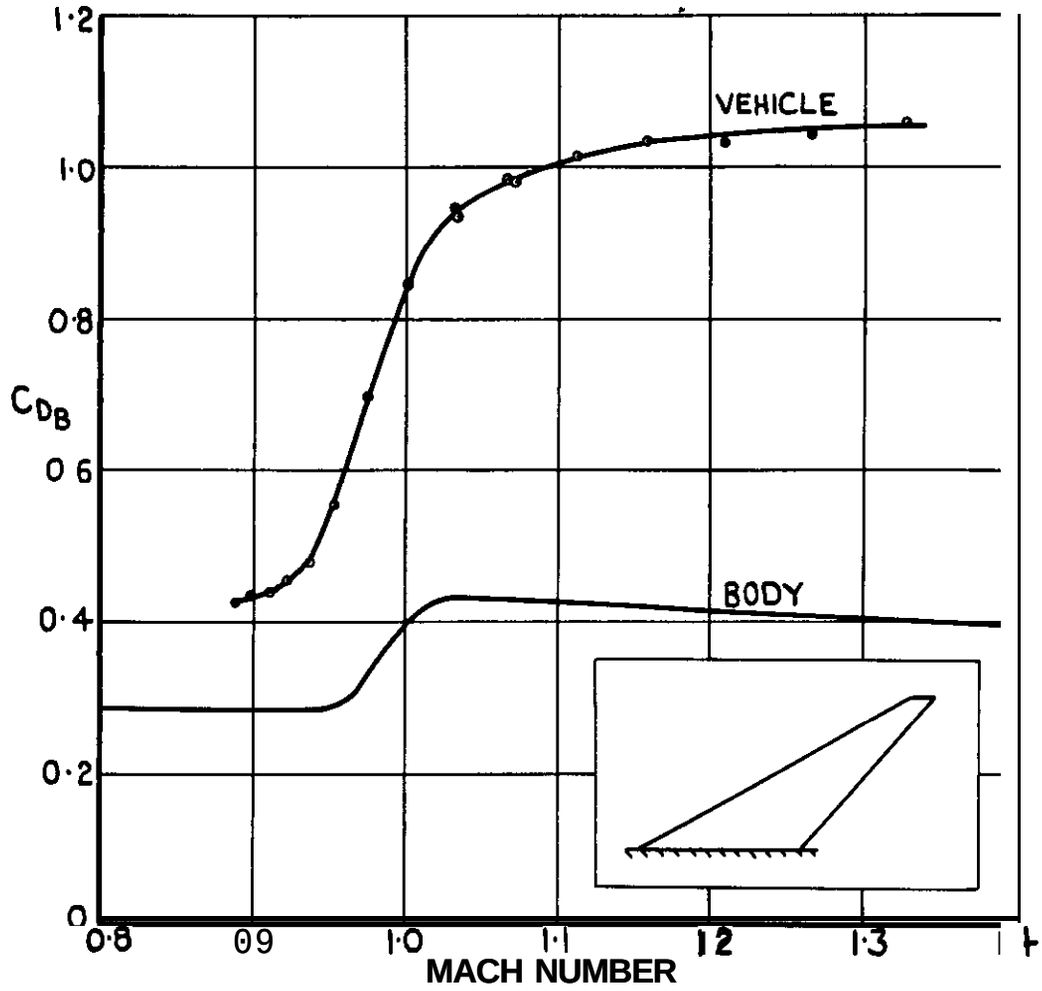

(a) DRAG BASED ON BODY FRONTAL AREA.

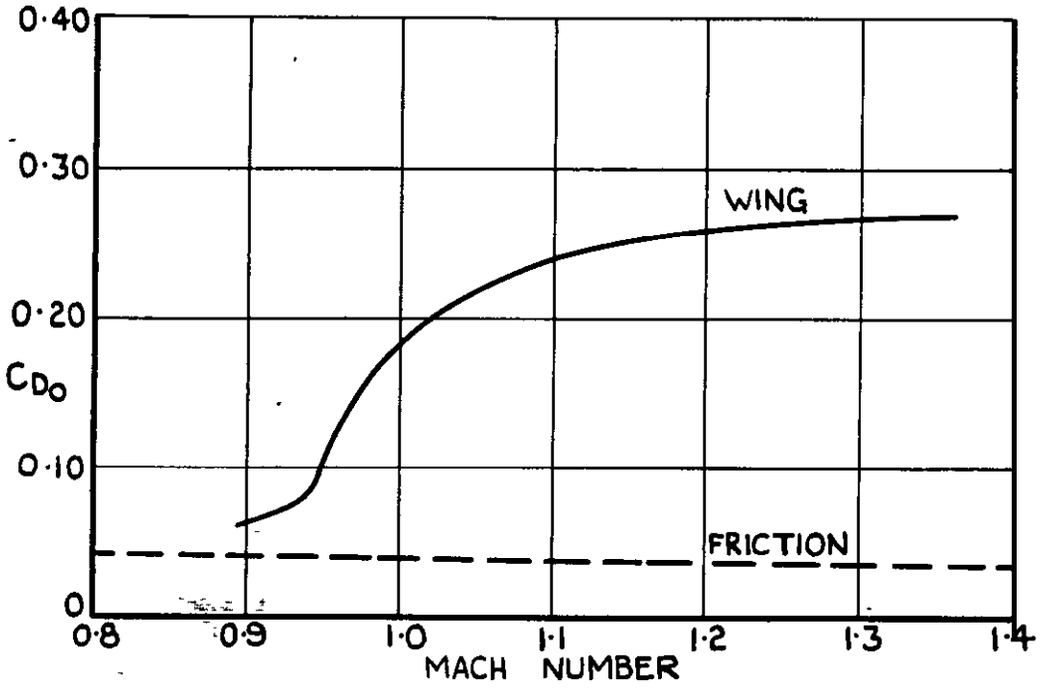

(b) DRAG BASED ON WING AREA.

FIG.18(a & b) DRAG OF MODEL 14.

FIG.19.(a.b & c)

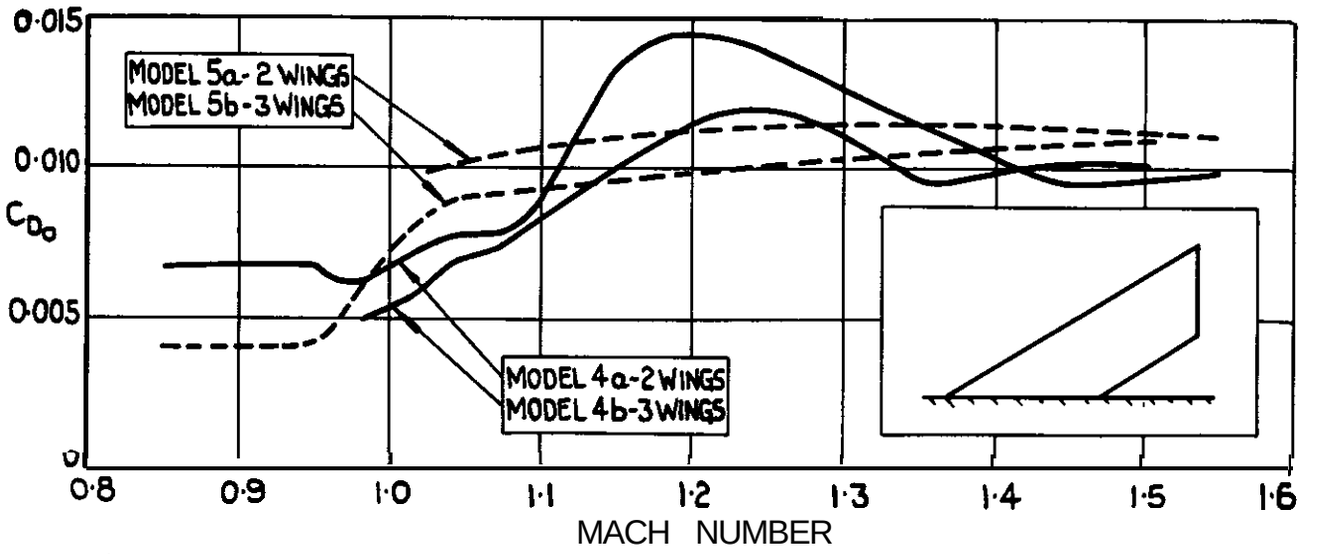

(a) MODELS 4 & 5.

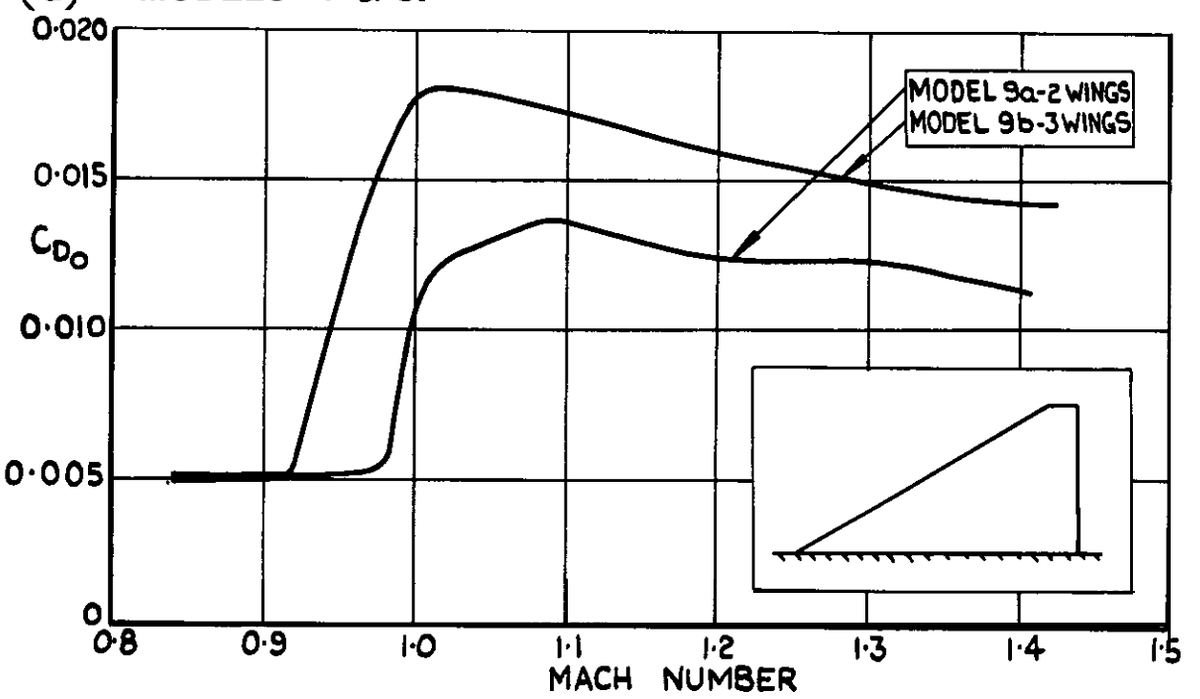

(b) MODEL 9.

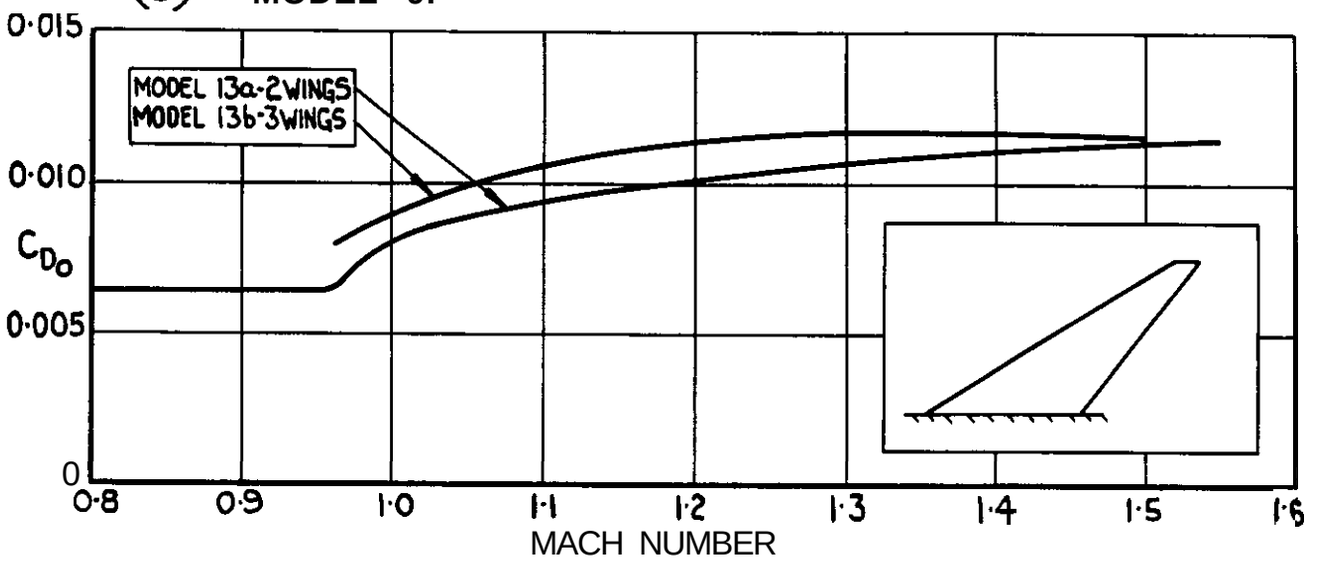

(c) MODEL 13.

FIG.19(a,b&c) COMPARISON OF DRAGS MEASURED ON 2 & 3-WING VEHICLES.

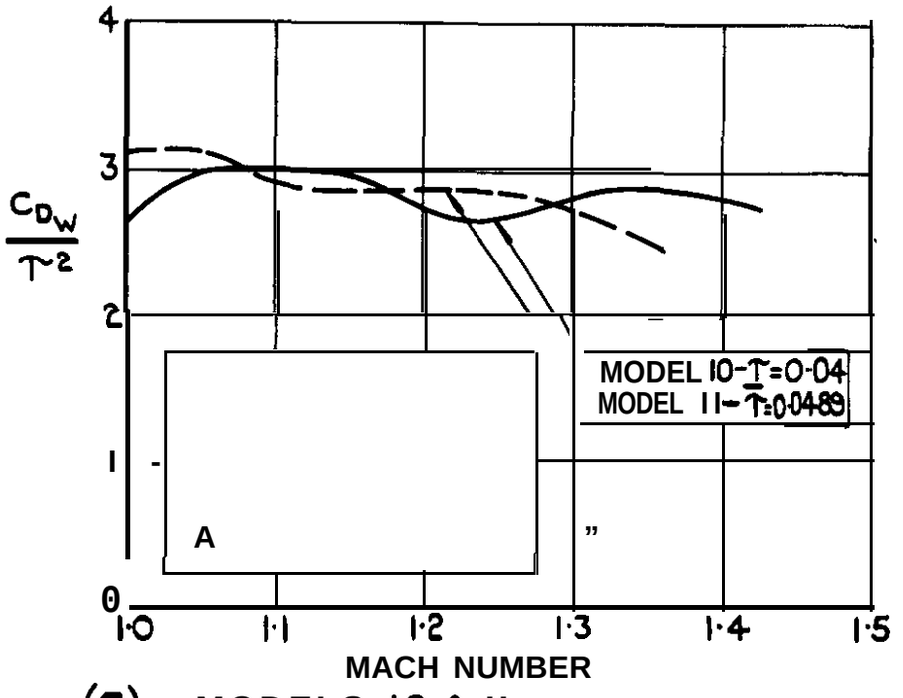

(a) MODELS 10 & 11.

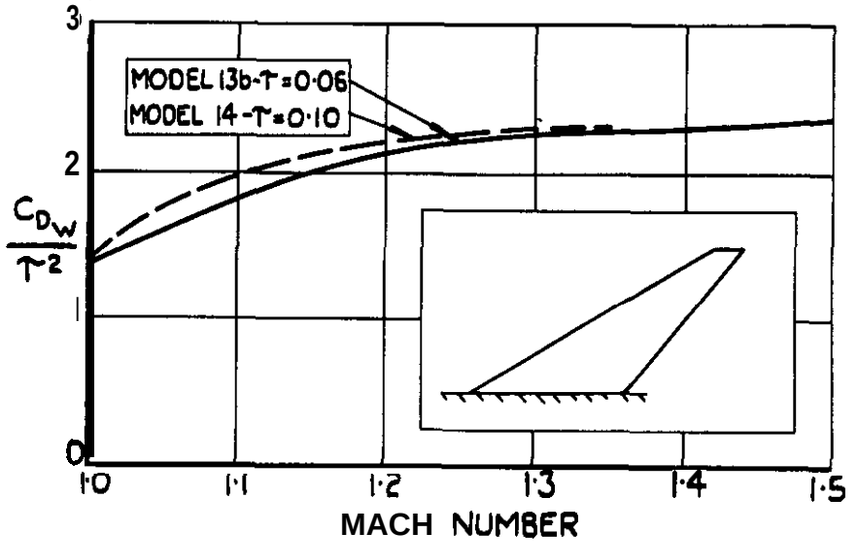

(b) MODELS 13 (b) & 14.

FIG. 20(a&b) EFFECT OF THICKNESS ON THE WAVE DRAG OF WINGS OF IDENTICAL PLANFORM.

FIG.21.

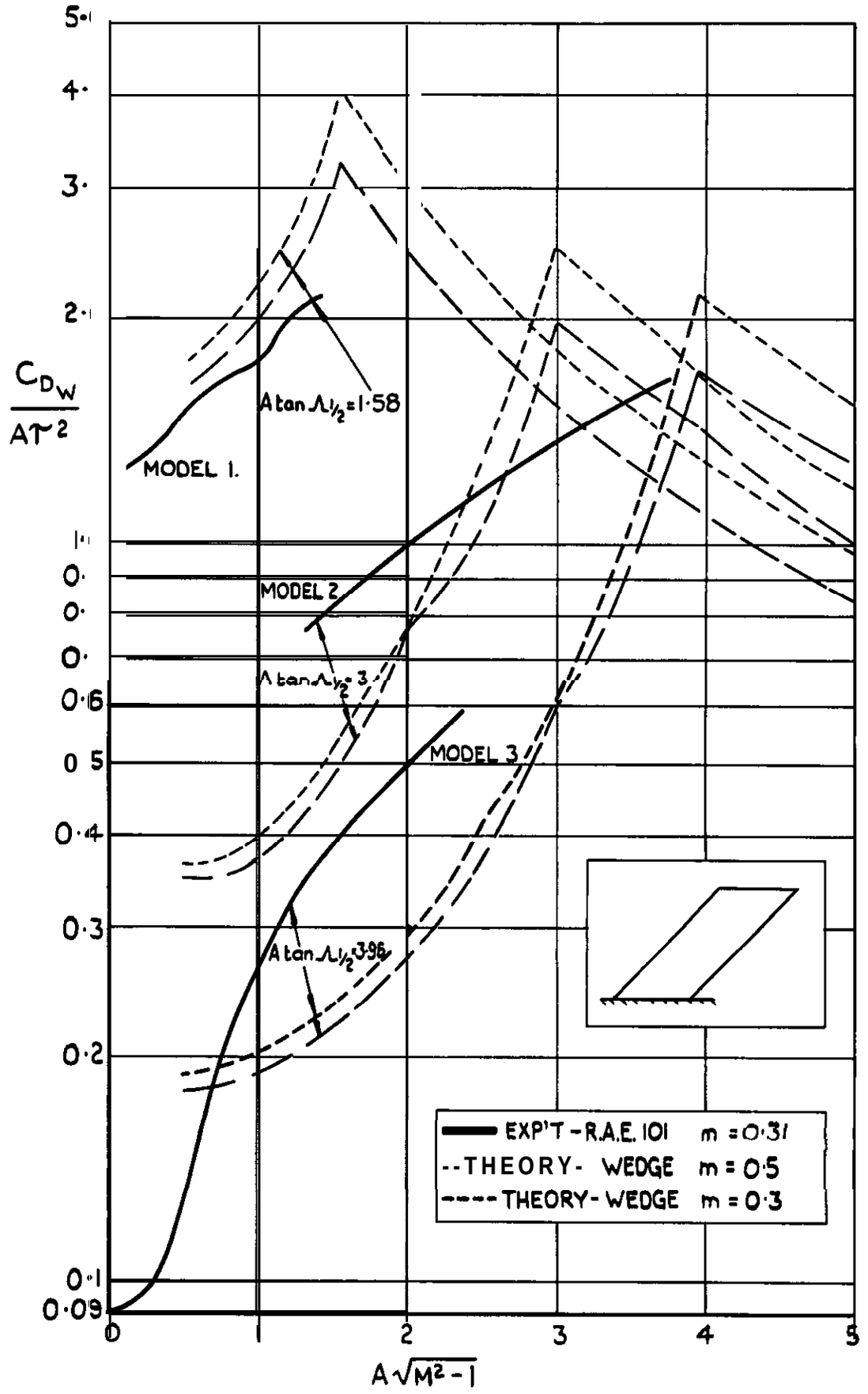

FIG.21. WAVE DRAG OF SWEPT UNTAPERED WINGS WITH STREAMWISE TIPS.

(THEORETICAL RESULTS FOR WINGS OF DOUBLE WEDGE SECTION SHOWN FOR COMPARISON)

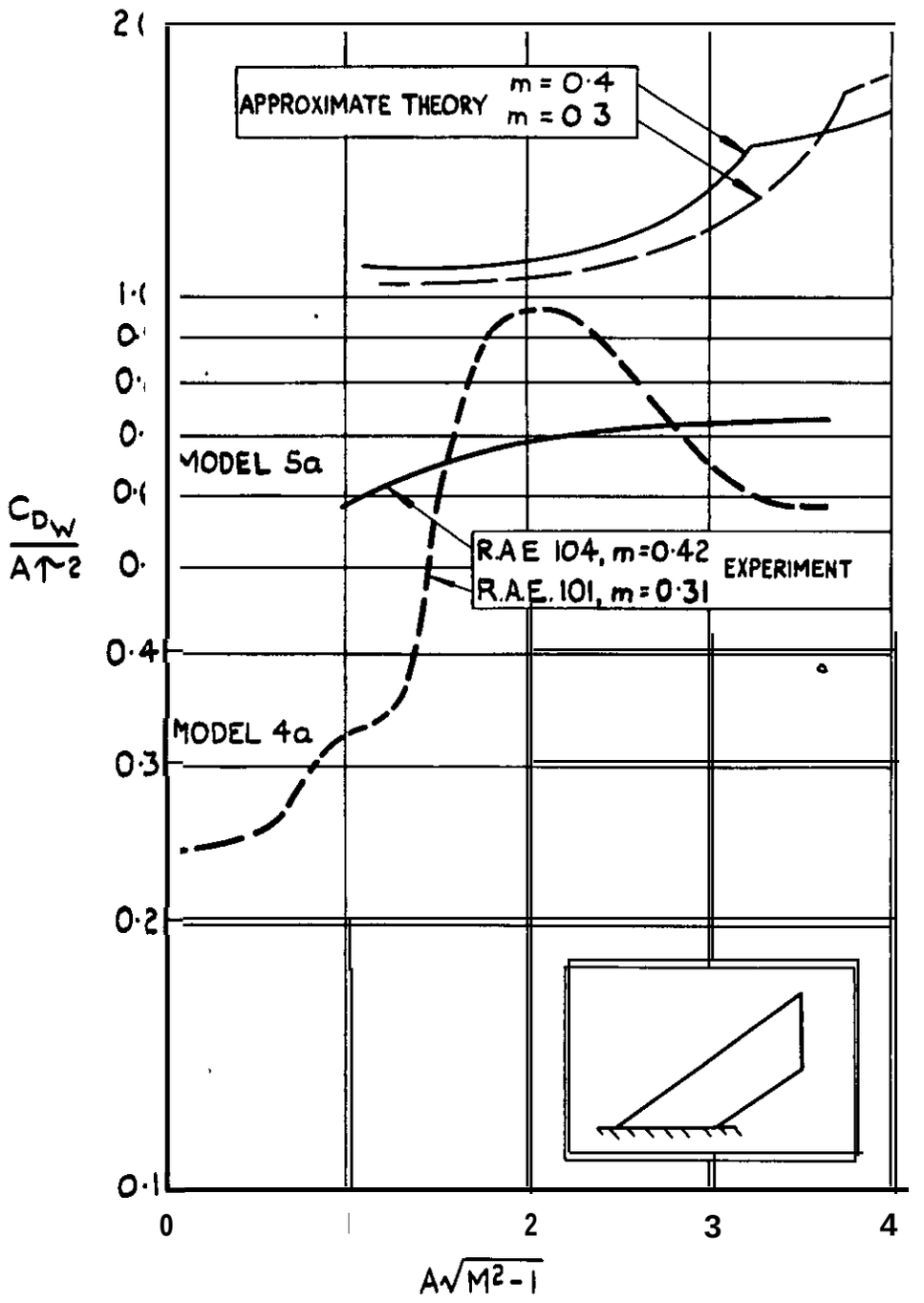

FIG.22.WAVE DRAG OF SWEPT UNTAPERED WINGS WITH CUT-OFF TIPS.

(THEORETICAL RESULTS FOR WINGS OF DOUBLE WEDGE SECTION SHOWN FOR COMPARISON.)

FIG.23 & 24.

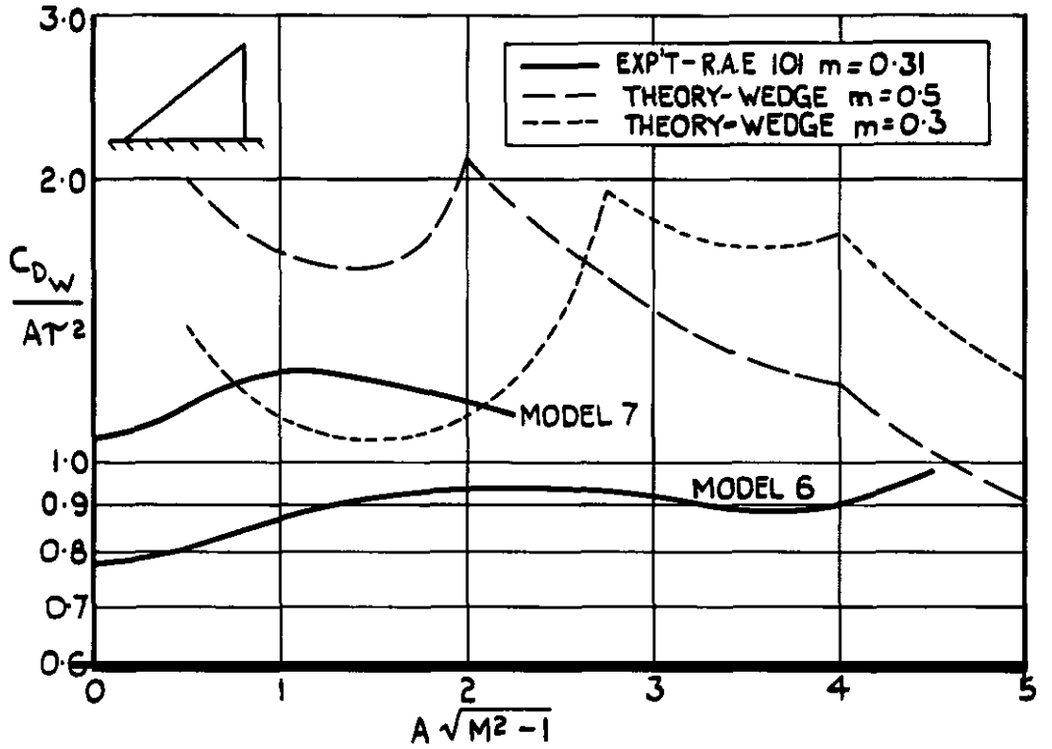

FIG.23. WAVE DRAG OF DELTA WINGS.

$A \tan \Lambda_{1/2} = 2, \quad \lambda = 0.$

(THEORETICAL RESULTS FOR WINGS OF DOUBLE WEDGE SECTION SHOWN FOR COMPARISON.)

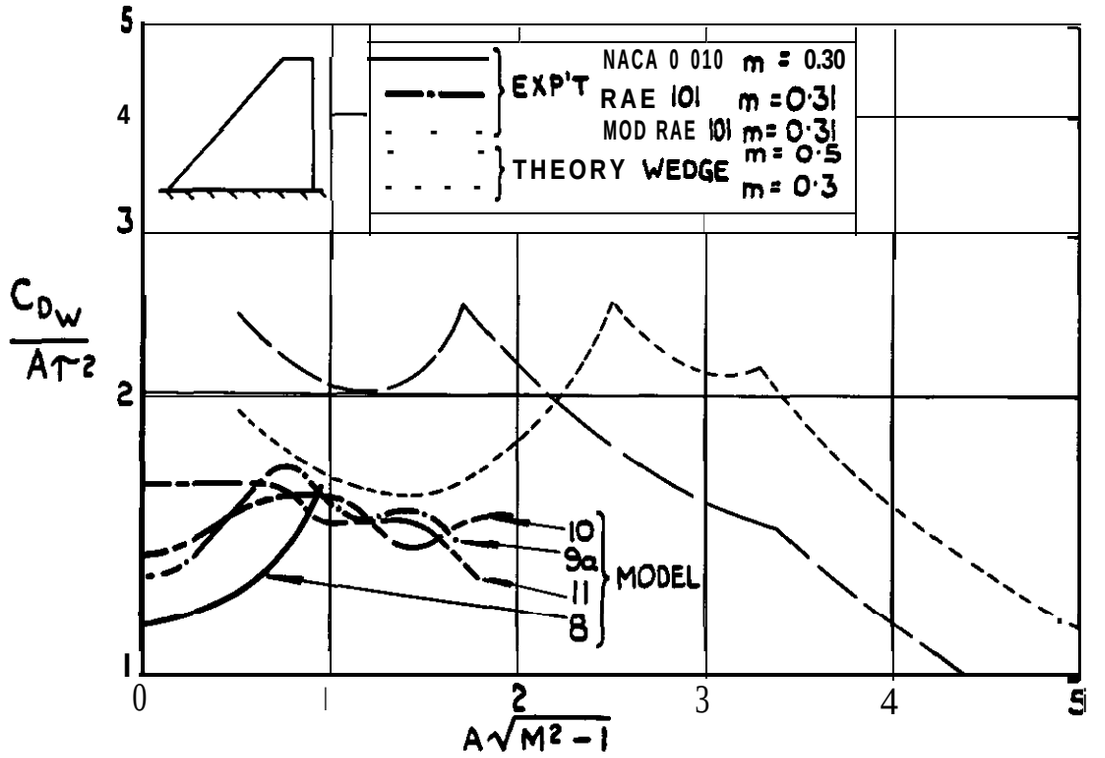

FIG.24. WAVE DRAG OF CROPPED DELTA WINGS.

(THEORETICAL RESULTS FOR WINGS OF DOUBLE WEDGE SECTION SHOWN FOR COMPARISON.)

MODEL	$A \tan \Lambda_{1/2}$	λ	m	SECTION
B	1·55	0·128	0·30	NACA 0010
9a	1·50	0·143	0·31	RAE 101-06
10	1·70	0·084	0.30	MODIFIED RAE 101
11				
THEORY	1·70	0·10	0·3,0·5	DOUBLE WEDGE

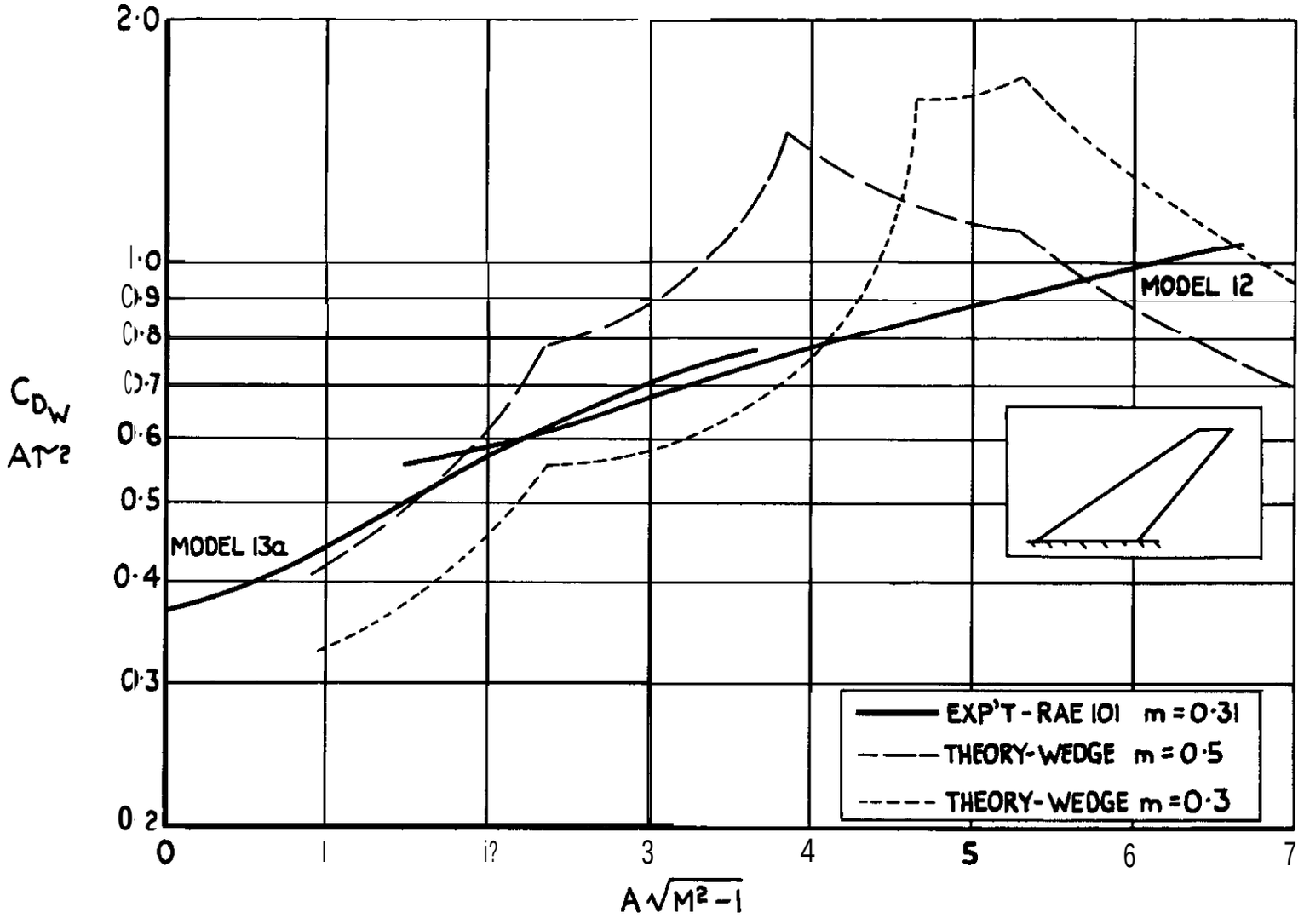

FIG.25 WAVE DRAG OF TAPERED WINGS WITH STREAMWISE TIPS.

A tan $\Lambda_{1/2}$ = 3.03, λ = 0·143.

(THEORETICAL RESULTS FOR WINGS OF DOUBLE WEDGE SECTION SHOWN FOR COMPARISON)

FIG.25.

C.P. No. 145
(15.243)
A.R.C. Technical Report

Crown Copyright Reserved

PUBLISHED BY HER MAJESTY'S STATIONERY OFFICE
To be purchased from
York House, Kingsway, LONDON, W c.2. 423 Oxford Street, LONDON, W 1
P 0 Box 569, LONDON, se I
13a Castle Street, EDINBURGH, 2 1 St Andrew's Crescent, CARDIFF
39 King Street, MANCHESTER, 2 Tower Lane. BRISTOL, I
2 Edmund Street, BIRMINGHAM, 3 80 Chichester street, BELFAST
or from any Bookseller
1954

Price 2s. 6d. net

PRINTED IN GREAT BRITAIN

S.O. Code No. U-9007-45